

## RESEARCH ARTICLE

# Canonical Wnt/ $\beta$ -catenin activity and differential epigenetic marks direct sexually dimorphic regulation of *Irx3* and *Irx5* in developing mouse gonads

Megan L. Koth<sup>1,†</sup>, S. Alexandra Garcia-Moreno<sup>2,†,\*</sup>, Annie Novak<sup>1</sup>, Kirsten A. Holthusen<sup>3</sup>, Anbarasi Kothandapani<sup>1</sup>, Keer Jiang<sup>1</sup>, Makoto Mark Taketo<sup>4</sup>, Barbara Nicol<sup>5</sup>, Humphrey H.-C. Yao<sup>5</sup>, Christopher R. Futtner<sup>2</sup>, Danielle M. Maatouk<sup>2,§</sup> and Joan S. Jorgensen<sup>1,¶</sup>

## ABSTRACT

Members of the Iroquois B (*IrxB*) homeodomain cluster genes, specifically *Irx3* and *Irx5*, are crucial for heart, limb and bone development. Recently, we reported their importance for oocyte and follicle survival within the developing ovary. *Irx3* and *Irx5* expression begins after sex determination in the ovary but remains absent in the fetal testis. Mutually antagonistic molecular signals ensure ovary versus testis differentiation with canonical Wnt/ $\beta$ -catenin signals paramount for promoting the ovary pathway. Notably, few direct downstream targets have been identified. We report that Wnt/ $\beta$ -catenin signaling directly stimulates *Irx3* and *Irx5* transcription in the developing ovary. Using *in silico* analysis of ATAC- and ChIP-Seq databases in conjunction with mouse gonad explant transfection assays, we identified TCF/LEF-binding sequences within two distal enhancers of the *IrxB* locus that promote  $\beta$ -catenin-responsive ovary expression. Meanwhile, *Irx3* and *Irx5* transcription is suppressed within the developing testis by the presence of H3K27me<sub>3</sub> on these same sites. Thus, we resolved sexually dimorphic regulation of *Irx3* and *Irx5* via epigenetic and  $\beta$ -catenin transcriptional control where their ovarian presence promotes oocyte and follicle survival vital for future ovarian health.

**KEY WORDS:**  $\beta$ -Catenin, Iroquois, Wnt, Enhancer, Epigenetics, Fetal gonad

## INTRODUCTION

Early in development, the bipotential mammalian gonad can transform into a testis or an ovary depending on the activation or repression of signaling cascades in the somatic cell lineage

(reviewed by Svingen and Koopman, 2013). In the ovary, the canonical Wnt4/Rspo1/ $\beta$ -catenin pathway plays a crucial role for proper differentiation and development (reviewed by Nicol and Yao, 2014). In XX mouse embryos, knockouts of *Wnt4* (Vainio et al., 1999; Jeays-Ward et al., 2004) and *Rspo1* (Chassot et al., 2008; Tomizuka et al., 2008), or somatic cell loss of their downstream mediator,  $\beta$ -catenin (Manuylov et al., 2008; Liu et al., 2009), results in a partial ovary to testis sex reversal and subsequent loss of 90% of the germ cell population by birth. Conversely, stabilization of  $\beta$ -catenin in the somatic cell population of the XY gonad leads to male-to-female sex reversal, suggesting that  $\beta$ -catenin is a crucial regulator of the sex identity of the somatic cell lineage (Maatouk et al., 2008). Multiple ovarian factors are thought to be regulated by  $\beta$ -catenin and its cognate DNA-binding partners TCF/LEF, but a direct relationship in the ovary has yet to be elucidated.

Previously, we reported that two Iroquois homeobox transcription factors *Irx3* and *Irx5* are expressed in the ovary, beginning shortly after sex differentiation. Each exhibits a dynamic profile during the course of germline nest establishment and breakdown through primordial follicle formation, suggesting they play important roles in ovarian development (Kim et al., 2011; Fu et al., 2018). Iroquois factors are highly conserved and are known for their roles in patterning and embryogenesis, along with organization of the spinal cord, limb, bone and heart (Bruneau et al., 2001; Diez del Corral et al., 1999; Gómez-Skarmeta et al., 2001; Gómez-Skarmeta and Modolell, 2002; Lovrics et al., 2014). Developmental regulation of these factors within these systems is context specific, as a number of signaling pathways have been described. Recently, we showed that null mutation of both *Irx3* and *Irx5* resulted in improper somatic-germ cell connections within follicles, which culminated in oocyte death (Fu et al., 2018). Notably, it has previously been reported that the *Wnt4* knockout mouse also exhibited physical gaps between germ and somatic cells within follicles (Vainio et al., 1999), suggesting that Wnt and Iroquois factors may lie in the same pathway. *Irx3* and *Irx5* expression have been attributed to the canonical Wnt signaling pathway in other tissues, including the developing mouse ovary (Naillat et al., 2010, 2015), but a direct link to  $\beta$ -catenin/TCF/LEF transcriptional regulation has not been made.

Based on results from our and other studies, we hypothesized that *Irx3* and *Irx5* are direct transcriptional targets of the canonical Wnt/ $\beta$ -catenin pathway in the developing ovary. We detected no sex-specific regulatory activity within the proximal promoter regions using *ex vivo* gonad transfection assays. Instead, we uncovered two distant regulatory sequences within the *IrxB* locus that promote sexually dimorphic expression during crucial stages of

<sup>1</sup>Department of Comparative Biosciences, School of Veterinary Medicine, University of Wisconsin – Madison, Madison, WI 53706, USA. <sup>2</sup>Department of Obstetrics and Gynecology, Northwestern University, Chicago, IL 60611, USA. <sup>3</sup>Department of Comparative Biosciences, College of Veterinary Medicine, University of Illinois, Urbana, IL 61802, USA. <sup>4</sup>Department of Pharmacology, Kyoto University Graduate School of Medicine, Kyoto 606-8501, Japan. <sup>5</sup>Reproductive and Developmental Biology Laboratory, National Institute of Environmental Health Sciences, Research Triangle Park, NC 27709, USA.

\*Present address: Department of Cell Biology, Duke University Medical Center, Durham, NC 27710, USA.

<sup>†</sup>These authors contributed equally to this work

<sup>§</sup>Deceased

<sup>¶</sup>Author for correspondence (joan.jorgensen@wisc.edu)

DOI: 10.1242/dev.183814. M.L.K., 0000-0003-3045-0101; A.N., 0000-0002-2595-6776; K.A.H., 0000-0002-8853-6066; A.K., 0000-0001-9701-0800; K.J., 0000-0001-6260-3796; M.M.T., 0000-0002-9032-4505; B.N., 0000-0002-3434-0658; H.H.-C.Y., 0000-0003-2944-8469; C.R.F., 0000-0003-3004-9983; J.S.J., 0000-0002-5787-8856

gonad differentiation. Herein, we report that active histone marks work together with  $\beta$ -catenin/TCF/LEF to bind and activate at least two enhancer regions within the *IrxB* locus to stimulate *Irx3* and *Irx5* transcription in the ovary. Meanwhile, these same sites were enriched for repressor H3K27me3 chromatin marks that actively repressed their transcription in developing testes. Together, these findings increase our perspective of the complex networks that are in place to ensure appropriate sex differentiation of gonads that include cooperation between epigenetic marks and transcription factors on promoter and distant regulatory sequences. In addition, this report uncovers mechanisms by which bipotential regulation can be achieved on the *IrxB* locus. These data provide a foundation for new discoveries of mechanisms by which canonical Wnt and other regulatory pathways work together to promote *IRX3* and *IRX5* function in a spatiotemporal manner within the developing ovary and during organogenesis of other systems, including the heart, limb, bone and spinal cord.

## RESULTS

### $\beta$ -Catenin activity correlates with *Irx3* and *Irx5* expression

Wnt4/Rspo1/ $\beta$ -catenin regulated transcription plays an essential role in ovarian development in somatic cells during sex differentiation. Our lab has previously reported that *Irx3* and *Irx5* expression increases upon the onset of sex differentiation in the ovary (Fu et al., 2018) and these factors have been linked to canonical Wnt/ $\beta$ -catenin signaling in other tissues (Janssens et al., 2010; Naillat et al., 2010, 2015). Therefore, we hypothesized that canonical  $\beta$ -catenin regulates *Irx3* and *Irx5* in the somatic cells of the ovary at this time. To test this hypothesis, *ex vivo* and *in vivo* approaches were used to manipulate  $\beta$ -catenin activity to cause loss- and gain-of-function in the developing mouse ovary and testis, respectively. Embryonic day 11.5 (E11.5) wild-type ovaries were dissected and then cultured for 24 h with two different doses of iCRT14, a small molecule that inhibits the interaction between  $\beta$ -catenin and TCF/LEF family members to block  $\beta$ -catenin-mediated gene transcription (Fig. 1A) (Yan et al., 2017; Gonsalves et al., 2011). As expected, treatment did

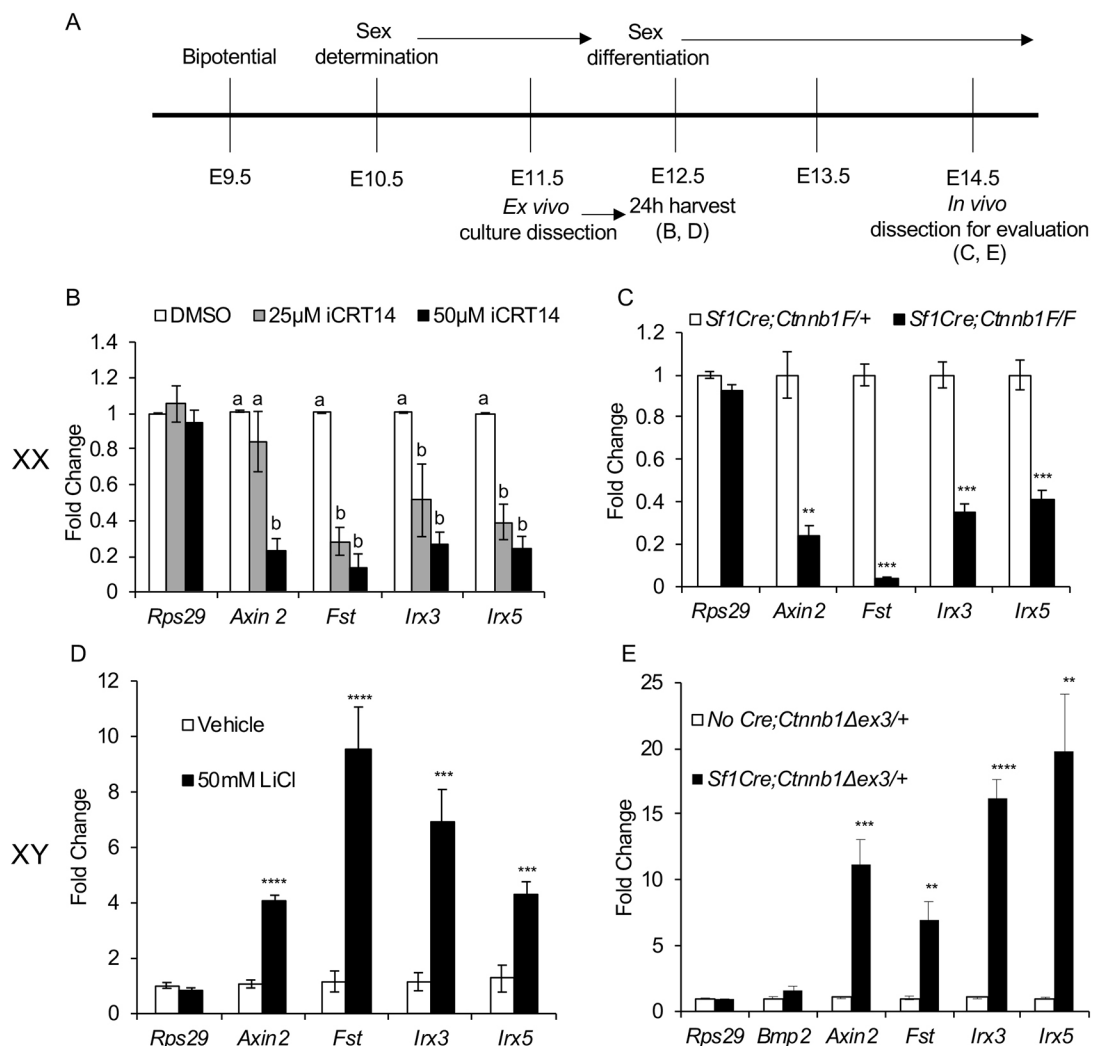


**Fig. 1.  $\beta$ -Catenin activity correlates with *Irx3* and *Irx5* expression.** (A) Experimental timeline for *ex vivo* and *in vivo* analysis of  $\beta$ -catenin manipulation in mouse gonads. Gonads first appear at embryonic day (E) 9.5 and sex determination commences by E10.5. (B) *Ex vivo*: RNA analysis from wild-type E11.5 ovaries (XX) that were cultured for 24 h in 20  $\mu$ l media containing either vehicle (DMSO), 25  $\mu$ M or 50  $\mu$ M iCRT14 ( $n=4$ ) [one-way ANOVA, post-hoc Tukey's comparison; different letters (a,b) represent significant differences ( $P<0.05$ ) between treatments within each condition]. (C) *In vivo*: RNA analysis of E14.5 ovaries (XX) from control (*Sf1Cre;Ctnnb1<sup>F/+</sup>*) and mutant (*Sf1Cre;Ctnnb1<sup>F/F</sup>*) embryos subjected to qPCR analysis ( $n=4-5$ ). (D) *Ex vivo*: RNA analysis of wild-type E11.5 testes (XY) cultured for 24 h in 20  $\mu$ l media containing either vehicle (water) or 50 mM lithium chloride (LiCl) ( $n=4$ ). (E) *In vivo*: RNA analysis of E14.5 testes (XY) from control (no Cre;*Ctnnb1<sup>Δex3/+</sup>*) and mutant (*Sf1Cre;Ctnnb1<sup>Δex3/+</sup>*) embryos subjected to qPCR analysis ( $n=6$ ). Data are mean $\pm$ s.e.m. Student's *t*-test, \*\* $P<0.01$ , \*\*\* $P<0.005$ , \*\*\*\* $P<0.001$ .



not change the expression of *Rps29*, a ribosomal protein used as a negative control, but inhibited  $\beta$ -catenin-responsive transcription in a dose-responsive manner. The 50  $\mu$ M dose decreased expression of known  $\beta$ -catenin target genes *Axin2* (77% decrease) and *Fst* (87% decrease), and caused a significant decrease in *Irx3* (73% decrease) and *Irx5* (76% decrease) transcripts (Fig. 1B). Next, we evaluated *Irx3* and *Irx5* transcript accumulation in embryonic ovaries lacking somatic cell  $\beta$ -catenin activity that were generated by crossing *SflCre* to *Ctnnb1<sup>F/F</sup>* mice (Fig. S1). *Rps29* transcripts from E14.5 control (*SflCre*; *Ctnnb1<sup>F/+</sup>*) and mutant (*SflCre*; *Ctnnb1<sup>F/F</sup>*) ovaries were not changed, whereas *Axin2* and *Fst* were significantly decreased in mutant ovaries (76% and 96% decreased, respectively). In support of the *ex vivo* culture findings, *Irx3* and *Irx5* transcripts were also significantly decreased (65 and 60% decreased, respectively) in the mutant ovaries compared with the controls (Fig. 1C). Together, *ex vivo* and *in vivo* results showed that the loss of  $\beta$ -catenin and its transcriptional activity in the developing ovary significantly diminished *Irx3* and *Irx5* expression.

Canonical Wnt/ $\beta$ -catenin is actively repressed in the developing testis (Kim et al., 2006; Uhlenhaut et al., 2009). Indeed, it has been shown that stabilization of  $\beta$ -catenin within the somatic cell population was sufficient to cause male-to-female sex reversal (Maatouk et al., 2008). Therefore, we evaluated whether  $\beta$ -catenin stabilization in the developing testis influenced *Irx3* and *Irx5* expression. Wild-type E11.5 testes were cultured *ex vivo* for 24 h with lithium chloride (LiCl) to stabilize  $\beta$ -catenin (Fig. 1A). Results from treated testes showed no change for *Rps29* and significantly increased expression of positive controls *Axin2* (fourfold) and *Fst* (10-fold). *Irx3* and *Irx5* transcripts also increased nine- and fivefold, respectively, compared to vehicle control (Fig. 1D). Previously it has been reported that stabilized  $\beta$ -catenin activity in somatic cells of developing testes from *SflCre*; *Ctnnb1<sup>Δex3/+</sup>* (Harada et al., 1999) embryos caused sex reversal (Maatouk et al., 2008). Transcripts from control (No Cre; *Ctnnb1<sup>Δex3/+</sup>*) and mutant (*SflCre*; *Ctnnb1<sup>Δex3/+</sup>*) testes (Fig. S1) at E14.5 displayed no significant change in *Rps29* transcript levels but exhibited significantly increased expression of *Axin2* (11-fold), *Fst* (7-fold), *Irx3* (16-fold) and *Irx5* (20-fold) (Fig. 1E). *Bmp2* was also used to test for Wnt/ $\beta$ -catenin specificity due to its role as a pro-ovarian gene that is not regulated by Wnt signaling.

Later in ovarian development, upon germline nest breakdown, *Irx3* expression expands to include both somatic cells and oocytes (Fu et al., 2018).  $\beta$ -Catenin is also present in oocytes at this stage as shown by our immunohistochemistry results from ovaries at E14.5 and P7 and supported by previous reports (Figs S1 and S2) (Yan et al., 2019; Bothun and Woods, 2019; Kumar et al., 2016; Usongo et al., 2012; Chassot et al., 2011; Jameson et al., 2012). To test whether  $\beta$ -catenin activity regulates expression of *Irx3* within oocytes post germline nest breakdown, we targeted loss of *Ctnnb1* in oocytes using *FiglaCre* (Lin et al., 2014) and evaluated ovaries at P0 and P7. Germ-cell-specific loss of  $\beta$ -catenin using *FiglaCre* was confirmed (Fig. S2A); however, immunohistochemistry analysis indicated no obvious change in *IRX3* within oocytes of mutant compared with control mice (Fig. S2B). Altogether, these data suggest that canonical  $\beta$ -catenin transcriptional activity promotes *Irx3* and *Irx5* expression within somatic cells of the germline nest but does not regulate their transcription within oocytes upon their appearance during germline nest breakdown.

#### **$\beta$ -Catenin responsive enhancer sites are present within the *IrxB* locus**

*Irx3* and *Irx5* are on opposing strands of DNA located 550 kb apart within the *IrxB* cluster on chromosome 8 in the mouse (Cavodeassi

et al., 2001; Peters et al., 2000). Given their proximity, we set out to identify accessible regions of chromatin within the *IrxB* locus. Previously, we performed DNaseI- and ATAC-seq on XY and XX somatic cell populations sorted from embryonic gonads at E10.5 (pre-sex determination) and E13.5 (post-sex determination) (Maatouk et al., 2017; Garcia-Moreno et al., 2019a). These datasets were used to interrogate chromosome 8 spanning 600 kb on either side of the *Irx3* transcription start site (TSS) to search for areas of open chromatin that also included the consensus motif for  $\beta$ -catenin-binding partners TCF/LEF (TCAAAG) (van de Wetering et al., 1997). The sites that were used for further evaluation included those that were either resolved (R) by or derived *de novo* (D) by E13.5 in the ovary (Garcia-Moreno et al., 2019a). Five sites of interest were identified and named based on their distances from the *Irx3* TSS: +205 kb, +86 kb, −305 kb (A,B) and −580 kb (see boxed peaks in Fig. 2). The site at −305 kb contained two separate TCF/LEF binding motifs, labeled 'A' and 'B'; all others harbored a single consensus element. A map detailing the approximate location of each site relative to *Irx3* and *Irx5* is outlined in Fig. 2.

To evaluate these open chromatin sites, we harvested ovaries and testes from E13.5–E14.5 embryos to perform chromatin immunoprecipitation (ChIP) qPCR using antibodies for H3K27ac to mark active enhancer sites, and TCF7L2 to identify TCF/LEF binding sites relevant to the developing ovary. Of TCF/LEF factors, TCF7L2 was chosen for the following reasons: robust ChIP-seq data are available on the ENCODE database; microarray data indicating TCF7L2 is expressed predominantly in the somatic cells of the gonad (Jameson et al., 2012); and the GUDMAP database shows that TCF7L2 expression is detected in the ovary via *in situ* hybridization, whereas other TCF/LEF factors are negative (Harding et al., 2011; McMahon et al., 2008). For each replicate, whole-gonad ChIP was first validated by showing RNA polymerase II enrichment at the GAPDH promoter and TCF7L2 presence at a known  $\beta$ -catenin/TCF complex target, the SP5 promoter (Kennedy et al., 2016), in ovaries and testes (Fig. S3). TCF7L2 and H3K27ac are present in other cells besides pre-granulosa cells; therefore, we anticipated variability in ChIP-PCR data from replicates sourced from whole-gonad tissue. Despite this potential barrier, our ChIP-PCR results showed substantial enrichment of H3K27ac and TCF7L2 binding on putative enhancer sequences in ovary (XX) compared with testis (XY) tissue (Fig. 3). Combined evaluation of H3K27ac and TCF7L2 results from ovary tissue suggest that  $\beta$ -catenin/TCF/LEF transcription factors bind and act on enhancer sequences at the +86 kb (H3K27ac 20.1-fold; TCF7L2 2.2-fold enrichment) and −580 kb (H3K27ac 11.1-fold; TCF7L2 2.7-fold enrichment) sites to regulate *Irx3* and *Irx5* expression within developing ovaries. These results also suggest the potential for sex-specific regulation.

#### **Constitutively active $\beta$ -catenin defines the +86 kb and −580 kb sites as Wnt responsive enhancers in the *IrxB* locus**

To test  $\beta$ -catenin responsive enhancer activity, each potential regulatory site was cloned into a luciferase reporter vector containing a minimal E1b promoter (Huang et al., 2006). In addition, each reporter vector was altered to include a single point mutation (in bold) of the TCF/LEF-binding motif (TCAAAG to CCAAAG), which is the same mutation that differentiates the TOPflash (active) versus FOPflash (inactive)  $\beta$ -catenin reporter plasmids (Korinek et al., 1997) (Table S1). Reporter plasmids were transfected into HEK293 cells along with a constitutively active  $\beta$ -catenin expression vector, CMV-S37A (Jordan et al., 2003). Specific  $\beta$ -catenin activity of the CMV-S37A expression

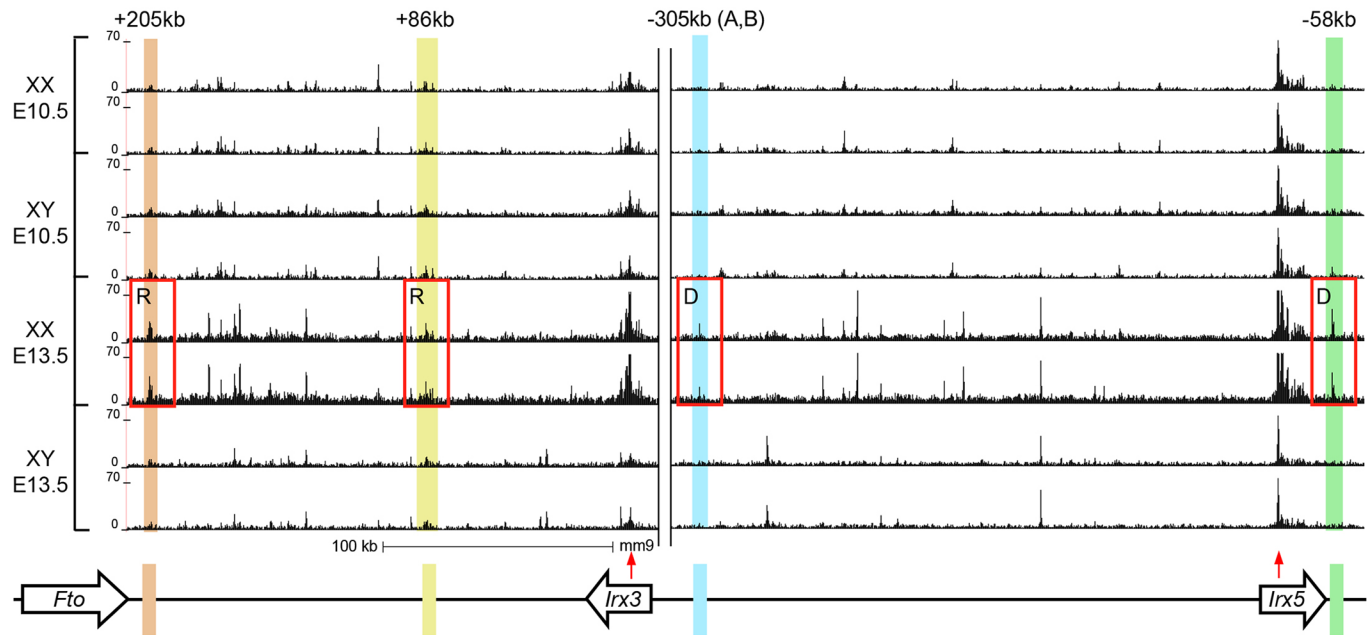


**Fig. 2. Open chromatin regions containing TCF/LEF-binding motifs are identified in the *Irx3* locus.** ATAC-seq tracks in isolated somatic cells pre (E10.5) and post (E13.5) sex determination from both female (XX) and male (XY) gonads show four highlighted regions that contain a female-specific peak at E13.5 and also includes a TCF/LEF-binding motif (TCAAAG) (outlined by red boxes). For each Seq analysis, there are duplicate assays presented for each age/sex gonad. Site -305 contains two separate TCF/LEF-binding motifs (A,B) that reside within 200 bp of each other within this peak. Each putative site is labeled based on its distance to the *Irx3* promoter. The positions of the TSSs of *Irx3* and *Irx5* are labeled with red arrows. Genes within the same locus include *Fto* and *Cmde* (lncRNA). Transcription direction is labeled with large arrows. A model of the *Irx3* locus and each putative enhancer site relative to the *Irx3* TSS is shown below the tracks. Color coding for each putative enhancer site is maintained throughout. R, resolved peaks; D, *de novo* peaks within the E13.5 ovary. ATAC-seq data were taken from Garcia-Moreno et al. (2019a).

vector was confirmed using co-transfection with positive and negative control reporter vectors, TOPflash and FOPflash, respectively (Fig. S4). Among all reporter vectors, including +250 kb, +86 kb, -305 kb (A,B) and -580 kb, only the +86 kb and -580 kb plasmids exhibited a significant increase in reporter activity that was specific to the putative TCF/LEF-binding site. Of note, the larger plasmid containing wild type -305 kb sequences, which includes A and B TCF/LEF binding sites, was not responsive to CMV-S37A, and the double mutation of A and B had no effect (Fig. 4A). To test whether the +86 kb and -580 kb DNA enhancers (together equals 209 bp) could stimulate promoter activity, both were cloned into the pGL3 basic luciferase reporter in front of 2080 bp of the mouse *Irx3* promoter (+86 kb; -580 kb; -1634/+446 bp *mIrx3* pGL3). Constitutively active CMV-S37A co-transfected with the enhancer plus promoter reporter stimulated a threefold increase in activity compared with promoter alone. In addition, single base pair point mutations of the TCF/LEF-binding site in each enhancer sequence completely disrupted enhancer activity (Fig. 4B). Together, these data suggest that the +86 kb and -580 kb enhancer sequences confer  $\beta$ -catenin-specific regulatory activity within the context of the *Irx3* promoter.

#### The +86 kb and -580 kb enhancers promote $\beta$ -catenin-specific activity in transfected fetal ovaries

Based on ovary-specific expression of *Irx3*, we reasoned that sequences within the *Irx3* promoter would confer ovary-specific expression. To test this hypothesis, three different sized segments of the mouse *Irx3* promoter (-351/+446 bp, -603/+446 bp and -1634/+446 bp) were cloned into a luciferase reporter plasmid and transfected into ovaries and testes from E13.5-E14.5 embryos (Fig. 5A). Although reporter activity increased along with longer promoter sequences, none of the promoters exhibited a significant

difference when testis and ovary reporter activities were compared (Fig. 5B). Next, we tested whether  $\beta$ -catenin-specific activity within the +86 kb and -580 kb enhancer sequences would promote ovary-specific expression. Both enhancers and their mutated counterparts were cloned in front of the most active promoter (-1634/+446 bp *mIrx3*pGL3) reporter vector and transfected into E14.5 gonads. Although the enhancer plus *mIrx3* promoter was equally expressed in both ovary and testes, only ovary expression was disrupted upon single basepair point mutations of the TCF/LEF-binding sites (60% decrease from wild-type enhancers) (Fig. 5C). Based on these results, we conclude that the +86 kb and -580 kb enhancer sequences promote  $\beta$ -catenin responsive activity only within the ovary.

#### The +86 kb and -580 kb regions in the testis are enriched for H3K27me3

Plasmid vectors containing the enhancer sequences linked to the mouse *Irx3* promoter did not confer ovary- versus testis-specific reporter activity, as expected; however, one limitation to this analysis is that plasmid reporter vectors lack epigenetic decorations that may have a profound impact on enhancer and/or promoter activity. Thus, we hypothesized that repressor histones suppress the +86 kb and -580 kb enhancer sequences within the developing testis. To test this hypothesis, we performed ChIP-Seq for the repressive histone modification H3K27me3 on FACS-purified XX and XY supporting cells from E13.5 gonads of *TESMS-CFP* (Gonen et al., 2018) and *Sox9-CFP* (Sekido and Lovell-Badge, 2008) transgenic mice, which fluorescently label granulosa (ovary) and Sertoli (testis) cells, respectively. Each ChIP-seq experiment was performed on two biological replicates containing pooled cells from multiple gonads. To maintain consistency, we performed ChIP-seq on the same somatic cell populations used for ATAC-seq

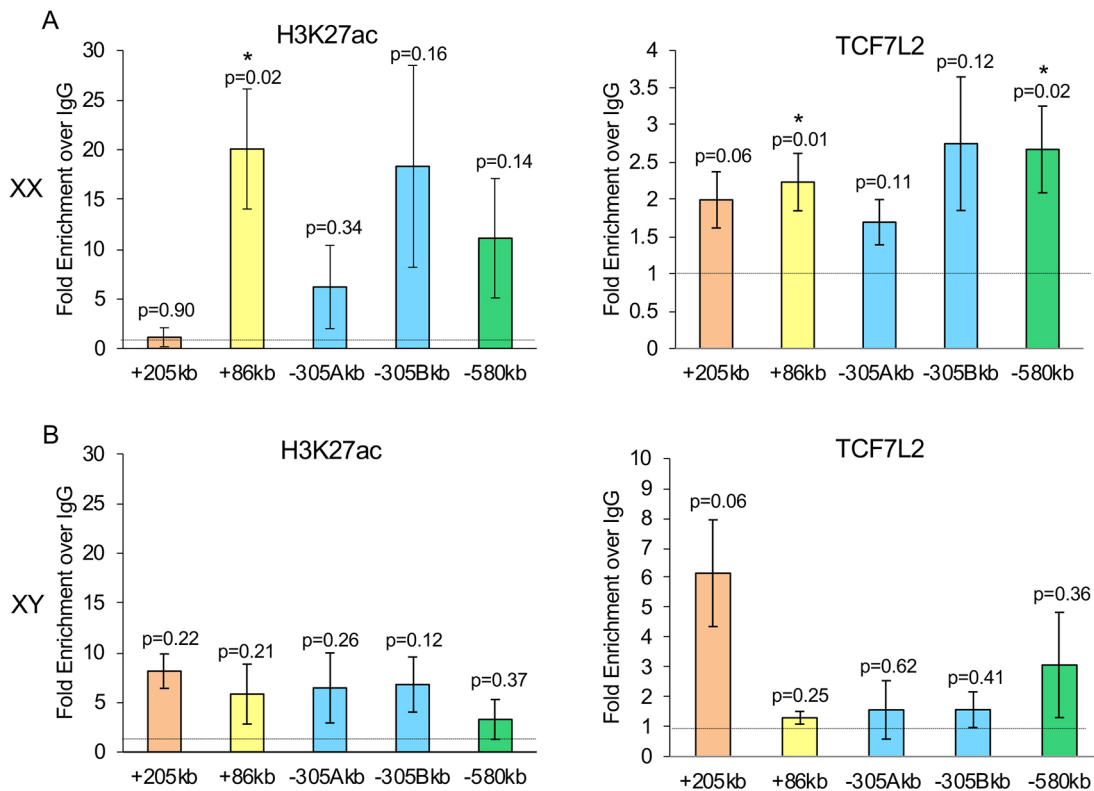


**Fig. 3. Ovary-specific  $\beta$ -catenin responsive enhancer sites reside within the *Irx5* locus.** (A) H3K27ac (active enhancer marker) (left panel) and  $\beta$ -catenin-binding partner TCF7L2 (right panel) chromatin immunoprecipitation (ChIP) of E14.5 ovaries (XX) from wild-type mice. (B) ChIP using the same markers in E14.5 testes (XY). H3K27ac (left panel) and TCF7L2 (right panel). Data are represented as mean fold change over IgG (which is normalized to 1)  $\pm$  s.e.m. Student's *t*-test. Female (XX), *n*=5-9; male (XY), *n*=3 or 4 biological replicates.

(Fig. 2). To validate our datasets, we compared our results with previously published H3K27me3 ChIP-seq (performed on the same somatic populations) and found high correlation among all four biological replicates (Fig. 6A). ChIP-seq data had previously been validated on promoters from genes known to drive sex determination and differentiation (Garcia-Moreno et al., 2019b). Results from ovary and testis H3K27me3 ChIP-seq are presented as peaks from individual replicates and include a solid horizontal bar above each set to illustrate the statistically positive sites, as

determined by HOMER analysis. Black vertical bars are included above these sites to illustrate positive ATAC-seq data. Results within the *Irx3/Irx5* locus show that H3K27me3 marks are enriched at each of the four selected sites in the Sertoli cells but are absent in granulosa cells. In contrast, ATAC-seq peaks are stronger in granulosa cells when compared with Sertoli cells (Fig. 6A). To illustrate the dynamic nature of epigenetic regulation that occurs during sex determination, we present a magnified view of the select sequences with a representative H3K27me3- and ATAC-seq

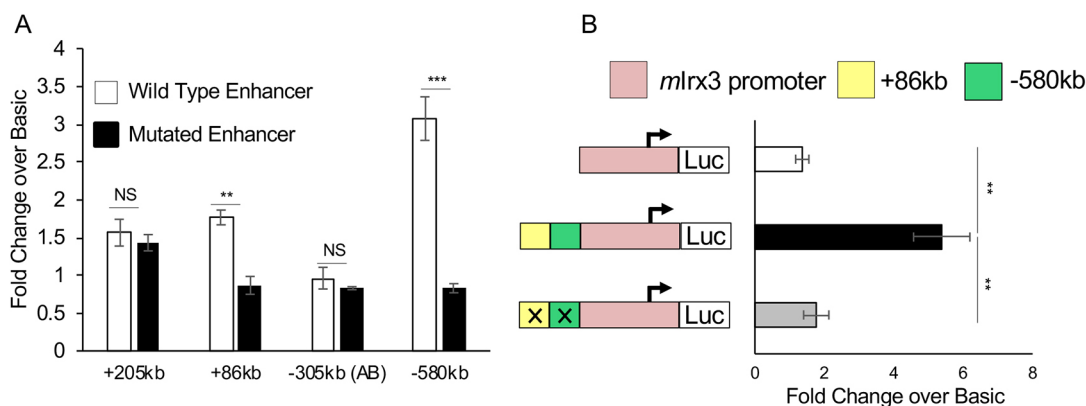


**Fig. 4. Constitutively active  $\beta$ -catenin defines the +86 kb and -580 kb enhancers as Wnt responsive within the *Irx3/5* locus.** (A) Luciferase reporter plasmids containing wild-type and mutated DNA sequences of each putative enhancer site were transfected into HEK293 cells along with CMV-S37A, an expression vector that encodes a constitutively active form of  $\beta$ -catenin. Test plasmids were normalized to pGL3 basic activity; *n*=3 individual experiments, each performed in triplicate. (B) -1634/+446 bp *mIrx3* pGL3 alone; +86 kb wild type, -580 kb wild type and -1634/+446 bp *mIrx3* pGL3; or +86 kb MUT; -580 kb MUT and -1634/+446 bp *mIrx3* pGL3 were transfected into HEK293 cells along with a constitutively active  $\beta$ -catenin expression vector, CMV-S37A. Data are mean  $\pm$  s.e.m.; *n*=4 or 5 individual experiments, each performed in triplicate. Student's *t*-test, \*\**P*<0.01, \*\*\**P*<0.005.

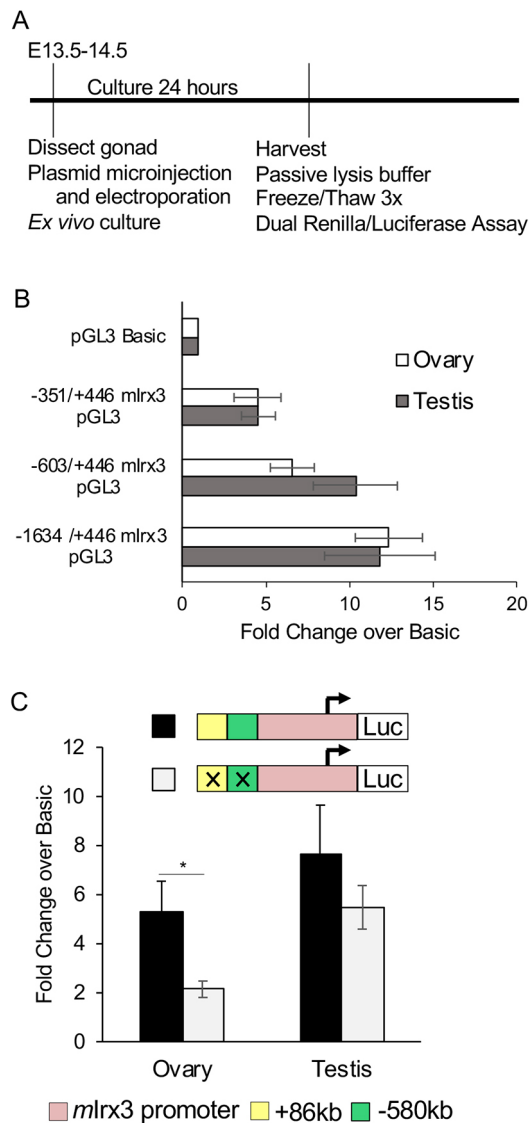


**Fig. 5. The +86 kb and -580 kb enhancers promote  $\beta$ -catenin-specific activity in transfected fetal ovaries.** (A) Experimental timeline for gonad dissection, transfection via microinjection and electroporation, and culture and harvest for dual luciferase assay. (B) Ex vivo transfections in ovary (white bars) versus testes (grey bars) of luciferase reporter vectors containing increasing sequence lengths of the mouse *lrx3* promoter (*lrx3* pGL3) compared with the empty pGL3 basic control reporter vector. -1634/+446 *lrx3* pGL3 testis,  $n=7$ ; ovary  $n=8$ ; -603/+446 testis *lrx3* pGL3,  $n=11$ ; ovary,  $n=8$ ; -351/+446 *lrx3* pGL3 testis and ovary,  $n=5$ . (C) Ex vivo transfections in ovary (white bars) versus testes (black bars) of wild-type enhancers +86 kb and -580 kb linked to -1634/+446 bp *lrx3* pGL3 or single base pair mutation (mut) enhancers mut+86 kb and mut-580 kb linked to -1634/+446 bp *lrx3* pGL3. Wild-type vector ovary,  $n=9$ ; wild-type vector testis,  $n=13$ ; MUT vector ovary,  $n=3$ ; MUT vector testis,  $n=7$ . Data are mean fold change over pGL3 basic  $\pm$  s.e.m. Student's *t*-test, \* $P<0.05$ .

replicates at E10.5 (pre-sex determination) and E13.5 (post-sex determination) in XX and XY supporting cells (Fig. 6B). Stage-dependent epigenetic control is evident at each enhancer site. At +205 kb, chromatin, which is initially accessible pre-sex determination, remains open in granulosa cells, whereas it transitions to a repressed and closed state in Sertoli cells at E13.5. At +86 kb, chromatin is initially open in both XX and XY at E10.5. At E13.5, accessibility increases and H3K27me3 decreases in granulosa cells, whereas H3K27me3 levels increase in the Sertoli

cells. Finally, closed chromatin at -306 kb and -580 kb, becomes accessible in granulosa cells at E13.5, whereas this site accumulates H3K27me3 in Sertoli cells.

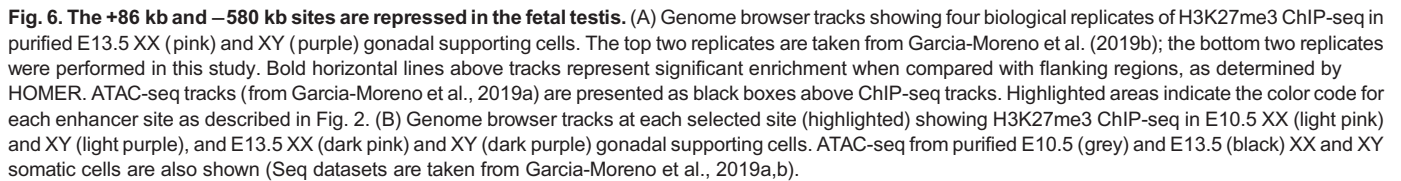
Taken together, our data uncovers two specific enhancers within the *lrx3* locus that confer ovary versus testis specific promoter activity. In the ovary, canonical  $\beta$ -catenin activity cooperates with active epigenetic marks on open chromatin to stimulate the +86 kb and -580 kb enhancers while expression is silenced in the testis due to the combined effects of histone methylation repression and the lack of functional  $\beta$ -catenin activity.

## DISCUSSION

Canonical Wnt/ $\beta$ -catenin signaling has been reported to promote *lrx3* and *lrx5* expression in the ovary (Naillat et al., 2010, 2015) and other tissues such as the brain (Braun et al., 2003), lung (Bell et al., 2008), neural axis (Janssens et al., 2010), kidney (Holmquist Mengelbier et al., 2019) and in colon cancer (Hovanes et al., 2001), but evidence for direct trans-acting regulation via DNA-binding partners has not been elucidated. Here, we used *in vitro*, *ex vivo* and *in vivo* approaches to provide a direct link between canonical Wnt/ $\beta$ -catenin signaling and *lrx3* and *lrx5* expression within the somatic cell population of the developing ovary. In addition, we previously showed that both Iroquois factors emerge in germ cells in late stages of ovarian development (Fu et al., 2018), but here we report that their regulation in this cell type is independent of  $\beta$ -catenin. Based on these data, we developed a model to describe regulation of *lrx3* and *lrx5* expression within the somatic cell population (Fig. 7). We uncovered two enhancer sequences that, although distant from the transcription start site, provide the focus for regulation within the ovary and testis. Our data indicate that chromatin enhancer marks work in conjunction with  $\beta$ -catenin/TCF/LEF at these sites to stimulate the *lrx3* locus in the ovary, while the absence of activated  $\beta$ -catenin in somatic cells along with repressive histone marks enriched at these same sites functionally antagonize expression of *lrx3* and *lrx5* in the testis. Together, these findings highlight interactions between signaling pathways and epigenetic marks that regulate *lrx3* and *lrx5* to ensure appropriate expression based on time, sex and cellular environments within developing gonads.

We examined ~1200 kb of chromosome 8, which included the *lrx3* and *Fto* loci, for female-specific open chromatin sites that could also mediate canonical  $\beta$ -catenin regulation within somatic cells after sex differentiation. Altogether, our DNase-Seq (Maatouk et al., 2017) and ATAC-Seq (Garcia-Moreno et al., 2019a) data, along with results from ENCODE ChIP-Seq derived TCF/LEF enrichment in human cell lines (ENCODE Project Consortium, 2012) illuminated five putative sites that met these criteria. Notably, none was identified within the proximal promoters of either *lrx3* or *lrx5*. One limitation of this study is that only perfect matches to the TCF/LEF-binding domains were explored. HMG box transcription factors, such as TCF/LEF, can also bind to DNA motifs that do not match the perfect consensus sequence; therefore, all potential binding regions were not explored. There were also several sex-specific sites of open chromatin within the *lrx3* locus that were not considered. Regarding the nucleosome-depleted regions that were evaluated in this study, JASPAR database interrogations uncovered a variety of other putative binding sites (Khan et al., 2018). These *in silico* analyses did not distinguish any common suite of transcription factor-binding sites within either the resolved or *de novo* open chromatin regions. In particular, the two sites that we identified as the most promising  $\beta$ -catenin-responsive enhancers in the ovary, +86 kb and -580 kb, were characterized as resolved and *de novo* sites, respectively. Besides TCF7L2, the +86 kb site harbors sequences that also bind CTCF,





elimination of  $\beta$ -catenin, suggest that chromatin encompassing the *IrxB* locus loops and undergoes extensive remodeling in response to sex-specific signals and developmental time.

The diagram illustrates the role of H3K27ac and H3K27me3 in gene expression. The top panel (female symbol) shows H3K27ac (green arrows) associated with active enhancers and promoters, leading to gene expression (green arrows). The bottom panel (male symbol) shows H3K27me3 (red dots) associated with repressed enhancers and promoters, leading to gene silencing (red T-bars).

DEVELOPMENT

of *Irx3* and *Irx5*. To that end, we combined traditional cell-based transfection assays with our previously described microinjection and electroporation technique to transfect reporter plasmids into embryonic gonads (Gao et al., 2011) with a specific focus on the mouse *Irx3* promoter (*mIrx3*-pGL3). We were surprised to find that the enhancer/*Irx3* promoter reporters were equally active in ovaries and testes. There are a number of potential reasons for this result. For example, it is recognized that reporter plasmid DNA transfection assays are used to focus attention to specific sequences, which are not in their normal context and, therefore, must be interpreted as such. In addition, plasmid DNA is devoid of epigenetic information, which has important implications on regulation. Indeed, our H3K27me3-Seq data show substantial enrichment at the proximal promoters of *Irx3* and *Irx5* only in XY cells (Fig. S5). Furthermore, our results showed that the response to mutation of the canonical TCF/LEF-binding site was not present in transfected testes, but was sensitive in cell and ovary transfection, both of which are  $\beta$ -catenin-responsive environments. Additional JASPAR analysis of the enhancer and promoter sequences uncovered several putative binding sites, including SOX, GATA, EZH2, CEBP and SP1 factors, among others. Together, these findings support the hypothesis that ovary-specific regulation for *Irx3* and *Irx5* is linked to canonical  $\beta$ -catenin signaling and opens the door for other means of regulation in the context of the loss of epigenetic marks that might explain high levels of testis reporter activity.

Because we expected reporter activity to be lower in transfected testes compared with ovaries, we evaluated the enhancer sites for histone repressor marks and found H3K27me3 marks were specifically enriched at +86 kb and -580 kb enhancer sites in addition to the proximal promoters of *Irx3* and *Irx5* in somatic cells of testes, but not ovaries. Thus, taken together, we conclude that both +86 kb and -560 kb open sites are subject to changing epigenetic landscapes. In newly differentiated ovarian somatic cells, active  $\beta$ -catenin/TCF complexes accumulate on the *IrxB* locus to stimulate *Irx3* and *Irx5* transcription. In contrast, somatic cells that are destined for the testis phenotype lack  $\beta$ -catenin and, instead, recruit epigenetic decorations consistent with transcriptional repression.

*Irx3* and *Irx5* show dynamic ovary-specific expression profiles (Fu et al., 2018). Besides canonical Wnt/ $\beta$ -catenin signaling, *Irx3* has also been shown to be controlled by other pathways, including TGF $\beta$  (Cavodeassi et al., 2001; Gómez-Skarmeta et al., 1998), SHH (Briscoe et al., 2000; Kobayashi et al., 2002), FGF (Kobayashi et al., 2002), and retinoic acid (Sirbu et al., 2005). Notably, many of these ligands have been established as sex-specific signals that also depend on a cadre of active transcription factors and epigenetic marks within the somatic cell population during the sex differentiation window (García-Moreno et al., 2018, 2019a; Katoh-Fukui et al., 2012; Hiramatsu et al., 2009; Morais da Silva et al., 1996). But important questions remain: which comes first and which regulates which? An interesting conundrum related to this question was illustrated in the evolving story of CBX2-mediated regulation of *Sry*. Originally, it was proposed that CBX2, a subunit of the canonical polycomb repressive complex 1 (PRC1) acted as a direct activator of *Sry* (Katoh-Fukui et al., 2012). New studies have since refined this discovery and now show that, within the developing testis, CBX2 and PRC1 establish repressor H3K27me3 marks to extinguish the rising profile of ovary pathway genes, which allows for accumulation of *Sry* (García-Moreno et al., 2019b). Other chromatin modifiers, including GLP-G9a/JMJD1 and CBP/p300, contribute to *Sry* expression by modulating H3K9Me2 repressor and H3K27ac marks (Kuroki

et al., 2013, 2017; Carré et al., 2018). These new data illustrate how epigenetic writers and readers can play a crucial role in sex determination and differentiation. Important insight can also be learned from species where sex determination is influenced by both genes and environmental cues. Indeed, there is a growing field in developmental epigenetics that increasingly recognizes that environmental cues are translated into specific sex phenotypes via epigenetic manipulations of sex determining genes (Navarro-Martín et al., 2011; Matsumoto et al., 2013; Parrott et al., 2014; Piferrer, 2013). Ultimately, plastic epigenetic marks provide flexibility and a means of preserving survival of sexually reproductive species.

The results of this study highlight the importance of transcription factor binding and local epigenetic landscape in illuminating cell and sex-defining fates during gonadogenesis. Distant enhancer sites have long been implicated in gene control in the gonad and new technologies are improving our capacity to identify and validate their importance (Sekido and Lovell-Badge, 2008; Gonen et al., 2018, 2017). Here, we describe two distal enhancer sites on the *IrxB* locus that are actively repressed in developing testes, while at the same time being engaged with active chromatin marks and  $\beta$ -catenin/TCF to stimulate *Irx3* and *Irx5* expression within the developing ovary. Thus, *Irx3* and *Irx5* are bona fide downstream targets of Wnt/Rspo1/ $\beta$ -catenin that, together, are crucial mediators of ovary development and oocyte survival. These findings allow us to begin to unravel the means by which specific cell environments control *Irx3* and *Irx5* expression within the fetal ovary. We suggest that these same principles could be applied to the developing brain, spinal cord, lung and kidney, or to abnormal cellular activity in Iroquois-positive cancers.

## MATERIALS AND METHODS

### Animals

Mouse strains included CD1 outbred mice [Crl:CD1(ICR), Charles River]; *Sf1*Cre mice (C57BL/6), originally obtained from the Keith Parker Lab (University of Texas Southwestern Medical Center) (Bingham et al., 2006); *Ctnnb1* conditional loss-of-function (LOF) mice (B6.129-*Ctnnb1*<sup>tm2Kem</sup>/KJWJ, Jackson Labs); and *Ctnnb1* conditional gain-of-function (GOF) mice (C57BL/6;  $\beta$ -cat<sup>fl,ex3</sup>), obtained from Dr Makoto Mark Taketo (Kyoto University, Kyoto, Japan) (Harada et al., 1999), *Sox9-CFP* (Sekido and Lovell-Badge, 2008) and *TESMS-CFP* (Gonen et al., 2018). Timed mating was identified by the presence of a vaginal plug, which was designated as embryonic day 0.5 (E0.5). Animals were dissected at the appropriate time and genomic DNA was isolated from tails or ear notches and subjected to PCR using gene-specific primers: *Sf1*Cre, 5'-GAGTGAACGAACCTGGTCA-AATCAGTGC-3' and 5'-GCATTACCGTGCATGCAACGAGTGATG-AG-3'; *Ctnnb1* wild-type and floxed (LOF) allele, 5'-AAGGTA-GAGTGATGAAAGTTGTT-3' and 5'-CACCATTGTCTCTGTCTATTCT-3'; and *Ctnnb1* wild-type and  $\beta$ -cat<sup>fl,ex3</sup> (GOF) allele, 5'-GCTGCGTGGA-CAATGGCTACTCAA-3' and 5'-GCCATGTCCAATCCATCAGGTCA-3'. In the case where sex could not be determined visually, PCR for SRY was performed using 5'-TGCAGCTCTACTCCAGTCTTG-3' and 5'-GATCTT-GATTTTGTAGTGTTC-3'.

Animal housing and all procedures described were reviewed and approved by the Institutional Animal Care and Use Committee at the University of Wisconsin-Madison and were performed in accordance with the National Institutes of Health Guiding Principles for the Care and Use of Laboratory Animals. Mice were housed in disposable, ventilated cages (Innovive). Rooms were maintained at 22±2°C and 30-70% humidity on a 12 h light/dark cycle.

### Organ culture using the droplet method

Gonad cultures were performed using a modified version of previously described protocols (Martineau et al., 1997; Maatouk et al., 2008). Briefly, E11.5 gonad/mesonephros complexes were cultured at 37°C with 5% CO<sub>2</sub>/95% air in ~20  $\mu$ l droplet of culture media [DMEM F-12 (Fisher,

SH3002301)] supplemented with 10% fetal bovine serum (Fisher, SH3091003) and 1% penicillin-streptomycin (Fisher, ICN1670249). The sex of the gonads was determined by genotyping PCR for SRY (see above). Gonad/mesonephros complexes were placed in round droplets of media on an inverted lid of a 100 mm Petri dish within a humidified chamber. Gonads (XX and XY) were cultured in a droplet supplemented with either vehicle control, the indicated concentrations of iCRT14 (XX gonads, Sigma SML0203) or LiCl (XY gonads, Fisher L121-100) for 24 h, rinsed with PBS and then harvested for RNA extraction and qPCR analysis.

### RNA extraction and qPCR

RNA was extracted using Trizol (Invitrogen, 15596026) according to the manufacturer's instructions and quantified using a NanoDrop 2000. RNA from each sample (500 ng) was used for First-Strand cDNA synthesis by SuperScriptII-RT (Invitrogen, AM9515). cDNA was diluted 1:5 and then 2 µl was added to 5 µl SYBR green PCR mixture (Applied Biosystems), 2.4 µl water and 1.25 pmol primer mix. PCR reactions were carried out using the ABI Prism 7000 Sequence Detection System (Applied Biosystems). RNA transcripts were quantified using the  $\Delta\Delta C_t$  method (Livak and Schmittgen, 2001). Briefly, to control for overall gene expression in each time point, the average cycle threshold (aveCt) for 36B4 was subtracted from the aveCt value for each gene to generate  $\Delta C_t$ . Next,  $\Delta C_t$  for each gene was compared with  $\Delta C_t$  of that same gene for the mutant genotype (e.g.  $\Delta C_t \text{ Irx3}_{\text{female control}} - \Delta C_t \text{ Irx3}_{\text{female mutant}}$ ) to generate  $\Delta\Delta C_t$ . Finally, fold-change was calculated as 2 to the  $-\Delta\Delta C_t$  power ( $2^{-\Delta\Delta C_t}$ ). Primers are listed in Table S2.

### DNase-I seq, ATAC-seq cluster analysis and ChIP-seq cluster analysis

DNase-I, ATAC-seq and H3K27me3 data were mined from previous studies (Maatouk et al., 2017; Garcia-Moreno et al., 2019a,b). These data were analyzed for open chromatin regions within 600 kb on either side of the *Irx3* transcription start site (TSS) of chromosome 8 in the mouse. Open chromatin regions that were specific to the granulosa cells after sex determination (E13.5) were explored for TCF/LEF-binding motifs using the JASPAR database (jaspar.genereg.net). The sequences containing the highest scores for binding potential were chosen for further investigation.

### Chromatin immunoprecipitation followed by qPCR

E13.5-E14.5 CD1 ovaries and testes without mesonephros were harvested, snap frozen and stored at  $-80^\circ\text{C}$ . 100-150 pairs of snap-frozen gonads were thawed and fixed in 1% formaldehyde for 15 min at room temperature with gentle shaking. The reaction was quenched with 160 µl of 1.25 M glycine for 5 min at room temperature with gentle shaking. Samples were washed twice with PBS and cComplete protease inhibitor (CPI) tablets (Roche, 04693116001) then resuspended in 400 µl RIPA lysis buffer+CPI tablets. Samples were homogenized with a pestle, then chromatin shearing was performed by lightly sonicating via probe-based sonication to fully lyse cells and the nuclear envelope followed by 1 min incubation at  $37^\circ\text{C}$  using 1000 gel units of Micrococcal Nuclease (MNase) (New England Biolabs, M0247S). A separate 5 µl sample was incubated with Proteinase K to validate efficient shearing of DNA (between 300 and 900 bp). The MNase reaction was stopped with 1.25 µmol EGTA. Debris was removed by centrifugation at  $15,000 g$  for 10 min at  $4^\circ\text{C}$  and then 100 µl of each lysate was diluted in 200 µl IP buffer (PBS+0.05% Triton X-100) and incubated overnight with 2 µg of antibody. After overnight antibody incubation, 25 µl of Dynabeads protein G magnetic beads (Life Technologies, 10004D) was added and mixed for 2 h at  $4^\circ\text{C}$  with gentle rocking. Samples were washed sequentially with 500 µl low salt, 500 µl high salt and 500 µl TE buffers, then resuspended in digestion buffer [50 mM Tris, 10 mM EDTA, 0.5% SDS (pH 8.0)] and proteinase K for 2 h at  $62^\circ\text{C}$ . DNA was isolated via ethanol precipitation. qPCR analysis was performed to quantify relative amounts of DNA enrichment; immunoprecipitated (IP) samples were normalized to input and IgG. Antibodies used were anti-phospho RNA PolII (Ser2) clone 3 (Millipore, MABE954), normal mouse IgG (Sigma, M8695), TCF4 (C4H811) (Cell Signaling Technology, 2569S) and Histone H3K27ac (Active Motif, 39133).

### Chromatin immunoprecipitation followed by next-generation sequencing

ChIP-seq was performed and analyzed as described by Garcia-Moreno et al. (2019b). Briefly, XX and XY supporting cells were FACS purified from E13.5 XY *SOX9-CFP* gonads and E13.5 XX *TESMS-CFP* gonads on the same day, and immediately processed for ChIP-seq. ChIP-seq was performed with no modifications (Van Galen et al., 2016) on two biological replicates, each containing ~150K FACS-purified supporting cells from pooled gonads. 400K *Drosophila* S2 cells were added per IP as carrier chromatin. ChIP-seq was performed using 3 µl of H3 antibody (Active Motif, 39763) (used as input) or 5 µl H3K27me3 antibody (CST, 9733S).

Sequence alignment to the mm9 mouse genome was performed using Bowtie. H3 ChIP-seq was used as input. To identify regions significantly enriched for H3K27me3 compared with flanking regions (peaks), HOMER was used for each independent replicate using the findPeaks function and settings '—style histone' and '—C 0', with a size of 5000. BigWig files were created using bedGraphToBigWig for visualization on the UCSC genome browser.

### Plasmid constructs

Luciferase reporters were generated from mouse genomic sequences of the enhancers at +205 kb, +86 kb, −305 kb and −580 kb from the *Irx3* transcription start site (TSS) specific to the region containing the TCF/LEF-binding motif via PCR with the addition of the KpnI and XhoI restriction enzyme sequences (Table S1). Each sequence was digested and inserted into the pGL3 basic vector containing a minimal E1b promoter (Huang et al., 2006) digested at the KpnI and XhoI sites. The QuikChangeII site-directed mutagenesis kit was used to make a single base pair mutation for each TCF/LEF-binding site, as directed in the manufacturer's protocol (Stratagene) (Table S1). The mouse *Irx3* promoter construct was generated from mouse genomic sequence using primers specific to 1634 bp upstream and 446 bp downstream of the *Irx3* TSS and placed into the pGL3 basic vector. The +86 kb and −580 kb sequences were inserted in front of the mouse *Irx3* promoter using the NEBuilder HiFi DNA Assembly Cloning Kit according to the manufacturer's instructions (New England BioLabs, E5520S). Each reporter construct was sequenced for accuracy after initial construction and proper mutation following mutagenesis (Sanger sequencing, UW Madison Biotech Center).

Plasmids containing promoter regions of *Irx3* were constructed via the Ensembl *Irx3* gene sequence and primer design software (Primer Designer version 1.01). PCR primers targeted the promoter region 5' of the *Irx3* TSS. Genomic DNA was amplified, and inserts were blunt-end ligated into the pST-blue Acceptor vector (Novagen). Sequencing was then performed (Keck Center, University of Illinois); the inserted sequence was compared with the archived DNA sequence (NT\_078586.1) and validated for accuracy.

### Cell culture and transient transfection

80,000 HEK293 cells (purchased from ATCC, CRL-1573, validated before shipment) were plated in 24-well plates (Thermo Scientific, 12565163) for transfection assays. Plasmids were prepped using column-based mini or midi prep kits (Qiagen, 27104, 12143) and quantified using a NanoDrop 2000. Cells were transfected using Lipofectamine 2000 (Invitrogen, 11668019) with plasmid DNA diluted in OPTI-MEM media (Fisher, 31985070) according to the manufacturer's instructions. Luciferase reporter vectors were transfected at 0.8 µg/well along with 50 ng/well co-expression vector CMV-EGFP (Addgene, 11153) or CMV-S37A-β-catenin (Jordan et al., 2003) (kindly provided by Dr Vincent Harley, Hudson Institute for Medical Research, Monash University, Melbourne, Australia) for normalization or treatment, respectively. The Lipofectamine 2000 mixture was incubated with the cells for 16-18 h followed by a media change. After 24 h, the cells were lysed using  $1\times$  passive lysis buffer and read using the Dual Luciferase Reporter Assay (Promega, E1910). Treatment groups were plated in triplicate and experiments were repeated at least three times. Luciferase values from the treatment group were normalized to the non-treatment group and also normalized to the empty vector control.



## Gonad injection and electroporation

Transient transfection assays in urogenital ridge explant cultures were based on previously reported methods of the explant culture system (Jorgensen and Gao, 2005). The sex of the gonad tissue was determined by characteristic findings of a coelomic vessel and testicular cords in the male and the lack of these in the female. Urogenital ridges were harvested from embryos at E14.5 and injected with ~0.5 µl of a DNA cocktail containing 4 µg/µl pGL3, wild-type +86 kb/−580 kb/Irx3 promoter pGL3 or mutated +86 kb/−580 kb/Irx3 promoter pGL3 plus 2 µg/µl SV40-Renilla luciferase in Dulbecco phosphate-buffered saline (PBS; Sigma D8537). An additional aliquot of 25 µl of sterile PBS was placed on the gonad for electroporation. Immediately thereafter, five square electrical pulses of 65 V, 50 ms each at 100 ms intervals, were delivered through platinum electrodes from an electroporator. After electroporation, urogenital ridges were placed back into the culture for 24 h. Explant cultures were maintained at 37°C with 5% CO<sub>2</sub>/95% air in 50 µl of Dulbecco minimal Eagle medium (DMEM) supplemented with 10% FBS (fetal bovine serum) and 1% penicillin/streptomycin. Transfected gonad explants were harvested in 50 µl passive lysis buffer, snap frozen, subjected to three freeze-thaw cycles and then processed for dual luciferase assays. Data were calculated by taking the ratio of luciferase to renilla expression with at least three biological replicates for each injected plasmid.

## Statistics

Statistics between groups were carried out using a two-tailed *t*-test assuming unequal variances. Results were considered statistically significant if  $P \leq 0.05$ . One-way ANOVA with a post-hoc Tukey's comparison was performed where appropriate.

## Acknowledgements

Special thanks to all members of the Jorgensen lab for ideas and support throughout this work, and to Drs John Svaren and Linda Schuler for extraordinary consultation. We are also extremely grateful for the technical support from Dr Camila Lopez-Anido and Dr John Svaren with our ChIP experiments. We also thank Janelle Ryan and Dr Vincent Harley for the CMV-S37A active  $\beta$ -catenin plasmid. We have an immense amount of gratitude to the cohort of undergraduates that helped with immunofluorescence, genotyping and sectioning, especially Linda Wang, Ann Turcotte and Rebekah Schroeder. In addition, we thank the University of Wisconsin Biotron for the exemplary mouse husbandry help. Dedicated to Danielle M. Maatouk, a wonderful colleague, scientist and friend.

## Competing interests

The authors declare no competing or financial interests.

## Author contributions

Conceptualization: M.L.K., S.A.G.-M., D.M.M., J.S.J.; Methodology: S.A.G.-M., D.M.M., J.S.J.; Validation: S.A.G.-M.; Formal analysis: M.L.K., S.A.G.-M., B.N., J.S.J.; Investigation: M.L.K., S.A.G.-M., A.N., K.A.H., A.K., K.J., B.N., H.H.-C.Y., C.R.F.; Resources: S.A.G.-M., M.M.T., H.H.-C.Y., D.M.M., J.S.J.; Data curation: S.A.G.-M., C.R.F., D.M.M.; Writing - original draft: M.L.K., S.A.G.-M., J.S.J.; Writing - review & editing: M.L.K., S.A.G.-M., M.M.T., B.N., H.H.-C.Y., J.S.J.; Visualization: M.L.K., S.A.G.-M., J.S.J.; Supervision: H.H.-C.Y., C.R.F., D.M.M., J.S.J.; Project administration: D.M.M., J.S.J.; Funding acquisition: H.H.-C.Y., D.M.M., J.S.J.

## Funding

This work was supported by the National Institutes of Health (R21HD48911, R01HD075079 and R01HD090660 to J.S.J.; R01HD090660-Reentry Supplement to A.K.; T32GM008688 to M.L.K.; and T32GM008061 to S.A.G.-M.). In addition, this research was also supported in part by the Intramural Research Program of the National Institutes of Health at the National Institute of Environmental Health Sciences (NIH-ZIAES102965 to H.H.-C.Y.). Deposited in PMC for release after 12 months.

## Data availability

The H3K27me3 ChIP-seq data have been deposited in GEO under accession number GSE146761.

## Supplementary information

Supplementary information available online at <http://dev.biologists.org/lookup/doi/10.1242/dev.183814.supplemental>

## Peer review history

The peer review history is available online at <https://dev.biologists.org/lookup/doi/10.1242/dev.183814.reviewer-comments.pdf>

## References

- Bell, S. M., Schreiner, C. M., Wert, S. E., Mucenski, M. L., Scott, W. J. and Whitsett, J. A. (2008). R-spondin 2 is required for normal laryngeal-tracheal, lung and limb morphogenesis. *Development* **135**, 1049–1058. doi:10.1242/dev.013359
- Bingham, N. C., Verma-Kurvari, S., Parada, L. F. and Parker, K. L. (2006). Development of a steroidogenic factor 1/Cre transgenic mouse line. *Genesis* **44**, 419–424. doi:10.1002/dvg.20231
- Bothun, A. M. and Woods, D. C. (2019). Dynamics of WNT signaling components in the human ovary from development to adulthood. *Histochem. Cell Biol.* **151**, 115–123. doi:10.1007/s00418-018-1729-y
- Braun, M. M., Etheridge, A., Bernard, A., Robertson, C. P. and Roelink, H. (2003). Wnt signaling is required at distinct stages of development for the induction of the posterior forebrain. *Development* **130**, 5579–5587. doi:10.1242/dev.00685
- Briscoe, J., Pierani, A., Jessell, T. M. and Ericson, J. (2000). A homeodomain protein code specifies progenitor cell identity and neuronal fate in the ventral neural tube. *Cell* **101**, 435–445. doi:10.1016/S0092-8674(00)80533-3
- Bruneau, B. G., Bao, Z.-Z., Fatkin, D., Xavier-Neto, J., Georgakopoulos, D., Maguire, C. T., Berul, C. I., Kass, D. A., Kuroski-De Bold, M. L., de Bold, A. J. et al. (2001). Cardiomyopathy in *Irx4*-deficient mice is preceded by abnormal ventricular gene expression. *Mol. Cell. Biol.* **21**, 1730–1736. doi:10.1128/MCB.21.5.1730-1736.2001
- Carré, G.-A., Siggers, P., Xipolita, M., Brindle, P., Lutz, B., Wells, S. and Greenfield, A. (2018). Loss of p300 and CBP disrupts histone acetylation at the mouse *Sry* promoter and causes XY gonadal sex reversal. *Hum. Mol. Genet.* **27**, 190–198. doi:10.1093/hmg/ddx398
- Cavodeassi, F., Modolell, J. and Gómez-Skarmeta, J. L. (2001). The Iroquois family of genes: from body building to neural patterning. *Development* **128**, 2847–2855.
- Chan, H. M. and La Thangue, N. B. (2001). p300/CBP proteins: HATs for transcriptional bridges and scaffolds. *J. Cell Sci.* **114**, 2363–2373.
- Chassot, A.-A., Ranc, F., Gregoire, E. P., Roepers-Gajadien, H. L., Taketo, M. M., Camerino, G., de Rooij, D. G., Schedl, A. and Chaboissier, M.-C. (2008). Activation of  $\beta$ -catenin signaling by *Rspo1* controls differentiation of the mammalian ovary. *Hum. Mol. Genet.* **17**, 1264–1277. doi:10.1093/hmg/ddn016
- Chassot, A.-A., Gregoire, E. P., Lavery, R., Taketo, M. M., de Rooij, D. G., Adams, I. R. and Chaboissier, M.-C. (2011). *RSPO1*/ $\beta$ -catenin signaling pathway regulates oogenesis differentiation and entry into meiosis in the mouse fetal ovary. *PLoS ONE* **6**, e25641. doi:10.1371/journal.pone.0025641
- Deng, Z., Cao, P., Wan, M. M. and Sui, G. (2010). Yin Yang 1: a multifaceted protein beyond a transcription factor. *Transcription* **1**, 81–84. doi:10.4161/trns.1.2.12375
- Diez del Corral, R., Aroca, P., Gomez-Skarmeta, J. L., Cavodeassi, F. and Modolell, J. (1999). The Iroquois homeodomain proteins are required to specify body wall identity in *Drosophila*. *Genes Dev.* **13**, 1754–1761. doi:10.1101/gad.13.13.1754
- ENCODE Project Consortium. (2012). An integrated encyclopedia of DNA elements in the human genome. *Nature* **489**, 57–74. doi:10.1038/nature11247
- Fu, A., Oberholtzer, S. M., Bagheri-Fam, S., Rastetter, R. H., Holdreith, C., Caceres, V. L., John, S. V., Shaw, S. A., Krentz, K. J., Zhang, X. et al. (2018). Dynamic expression patterns of *Irx3* and *Irx5* during germline nest breakdown and primordial follicle formation promote follicle survival in mouse ovaries. *PLoS Genet.* **14**, e1007488. doi:10.1371/journal.pgen.1007488
- Gao, L., Kim, Y., Kim, B., Lofgren, S. M., Schultz-Norton, J. R., Nardulli, A. M., Heckert, L. L. and Jorgensen, J. S. (2011). Two regions within the proximal steroidogenic factor 1 promoter drive somatic cell-specific activity in developing gonads of the female mouse. *Biol. Reprod.* **84**, 422–434. doi:10.1095/biolreprod.110.084590
- Garcia-Moreno, S. A., Plebanek, M. P. and Capel, B. (2018). Epigenetic regulation of male fate commitment from an initially bipotential system. *Mol. Cell. Endocrinol.* **468**, 19–30. doi:10.1016/j.mce.2018.01.009
- Garcia-Moreno, S. A., Futtner, C. R., Salamone, I. M., Gonen, N., Lovell-Badge, R. and Maatouk, D. M. (2019a). Gonadal supporting cells acquire sex-specific chromatin landscapes during mammalian sex determination. *Dev. Biol.* **446**, 168–179. doi:10.1016/j.ydbio.2018.12.023
- Garcia-Moreno, S. A., Lin, Y.-T., Futtner, C. R., Salamone, I. M., Capel, B. and Maatouk, D. M. (2019b). CBX2 is required to stabilize the testis pathway by repressing Wnt signaling. *PLoS Genet.* **15**, e1007895. doi:10.1371/journal.pgen.1007895
- Ghirlando, R. and Felsenfeld, G. (2016). CTCF: making the right connections. *Genes Dev.* **30**, 881–891. doi:10.1101/gad.277863.116
- Gómez-Skarmeta, J. L. and Modolell, J. (2002). Iroquois genes: genomic organization and function in vertebrate neural development. *Curr. Opin. Genet. Dev.* **12**, 403–408. doi:10.1016/S0959-437X(02)00317-9
- Gómez-Skarmeta, J. L., Glavic, A., de la Calle-Mustienes, E., Modolell, J. and Mayor, R. (1998). Xiro, a *Xenopus* homolog of the *Drosophila* Iroquois complex genes, controls development at the neural plate. *EMBO J.* **17**, 181–190. doi:10.1093/embioj/17.1.181
- Gómez-Skarmeta, J., de la Calle-Mustienes, E. and Modolell, J. (2001). The Wnt-activated Xiro1 gene encodes a repressor that is essential for neural



- development and downregulates Bmp4. *Development* **128**, 551–560. doi:10.3410/f.1002239.9110
- Gonen, N., Quinn, A., O'Neill, H. C., Koopman, P. and Lovell-Badge, R. (2017). Normal levels of Sox9 expression in the developing mouse testis depend on the TES/ESCO enhancer, but this does not act alone. *PLoS Genet.* **13**, e1006520. doi:10.1371/journal.pgen.1006520
- Gonen, N., Futtner, C. R., Wood, S., Garcia-Moreno, S. A., Salamone, I. M., Samson, S. C., Sekido, R., Poulat, F., Maatouk, D. M. and Lovell-Badge, R. (2018). Sex reversal following deletion of a single distal enhancer of Sox9. *Science* **360**, 1469–1473. doi:10.1126/science.aas9408
- Gonsalves, F. C., Klein, K., Carson, B. B., Katz, S., Ekas, L. A., Evans, S., Nagourney, R., Cardozo, T., Brown, A. M. C. and Dasgupta, R. (2011). An RNAi-based chemical genetic screen identifies three small-molecule inhibitors of the Wnt/wingless signaling pathway. *Proc. Natl. Acad. Sci. USA* **108**, 5954–5963. doi:10.1073/pnas.1017496108
- Harada, N., Tamai, Y., Ishikawa, T., Sauer, B., Takaku, K., Oshima, M. and Taketo, M. M. (1999). Intestinal polyposis in mice with a dominant stable mutation of the beta-catenin gene. *EMBO J.* **18**, 5931–5942. doi:10.1093/emboj/18.21.5931
- Harding, S. D., Armit, C., Armstrong, J., Brennan, J., Cheng, Y., Haggarty, B., Houghton, D., Lloyd-Macgilp, S., Pi, X., Roochun, Y. et al. (2011). The GUDMAP database—an online resource for genitourinary research. *Development* **138**, 2845–2853. doi:10.1242/dev.063594
- Hiramatsu, R., Matoba, S., Kanai-Azuma, M., Tsunekawa, N., Katoh-Fukui, Y., Kurohmaru, M., Morohashi, K.-I., Wilhelm, D., Koopman, P. and Kanai, Y. (2009). A critical time window of Sry action in gonadal sex determination in mice. *Development* **136**, 129–138. doi:10.1242/dev.029587
- Holmquist Mengelbier, L., Lindell-Munther, S., Yasui, H., Jansson, C., Esfandyari, J., Karlsson, J., Lau, K., Hui, C.-C., Bexell, D., Hopyan, S. et al. (2019). The Iroquois homeobox proteins IRX3 and IRX5 have distinct roles in Wilms tumour development and human nephrogenesis. *J. Pathol.* **247**, 86–98. doi:10.1002/path.5171
- Hovanes, K., Li, T. W. H., Munguia, J. E., Truong, T., Milovanovic, T., Lawrence Marsh, J., Holcombe, R. F. and Waterman, M. L. (2001). Beta-catenin-sensitive isoforms of lymphoid enhancer factor-1 are selectively expressed in colon cancer. *Nat. Genet.* **28**, 53–57. doi:10.1038/ng0501-53
- Huang, M., Jia, F.-J., Yan, Y.-C., Guo, L.-H. and Li, Y.-P. (2006). Transactivated minimal E1b promoter is capable of driving the expression of short hairpin RNA. *J. Virol. Methods* **134**, 48–54. doi:10.1016/j.jviromet.2005.11.016
- Jameson, S. A., Natarajan, A., Cool, J., Defalco, T., Maatouk, D. M., Mork, L., Munger, S. C. and Capel, B. (2012). Temporal transcriptional profiling of somatic and germ cells reveals biased lineage priming of sexual fate in the fetal mouse gonad. *PLoS Genet.* **8**, e1002575. doi:10.1371/journal.pgen.1002575
- Janssens, S., Denayer, T., Deroo, T., VAN Roy, F. and Vleminckx, K. (2010). Direct control of Hoxd1 and Irx3 expression by Wnt/beta-catenin signaling during anteroposterior patterning of the neural axis in *Xenopus*. *Int. J. Dev. Biol.* **54**, 1435–1442. doi:10.1387/jidb.092985sj
- Jeays-Ward, K., Dandonneau, M. and Swain, A. (2004). Wnt4 is required for proper male as well as female sexual development. *Dev. Biol.* **276**, 431–440. doi:10.1016/j.ydbio.2004.08.049
- Jordan, B. K., Shen, J. H.-C., Olaso, R., Ingraham, H. A. and Vilain, E. (2003). Wnt4 overexpression disrupts normal testicular vasculature and inhibits testosterone synthesis by repressing steroidogenic factor 1/ $\beta$ -catenin synergy. *Proc. Natl. Acad. Sci. USA* **100**, 10866–10871. doi:10.1073/pnas.1834480100
- Jorgensen, J. S. and Gao, L. (2005). Irx3 is differentially up-regulated in female gonads during sex determination. *Gene Expr. Patterns* **5**, 756–762. doi:10.1016/j.modgep.2005.04.011
- Katoh-Fukui, Y., Miyabayashi, K., Komatsu, T., Owaki, A., Baba, T., Shima, Y., Kidokoro, T., Kanai, Y., Schedl, A., Wilhelm, D. et al. (2012). Cbx2, a polycomb group gene, is required for Sry gene expression in mice. *Endocrinology* **153**, 913–924. doi:10.1210/en.2011-1055
- Kennedy, M. W., Chalamalasetty, R. B., Thomas, S., Garriock, R. J., Jailwala, P. and Yamaguchi, T. P. (2016). Sp5 and Sp8 recruit  $\beta$ -catenin and Tcf1-Lef1 to select enhancers to activate Wnt target gene transcription. *Proc. Natl. Acad. Sci. USA* **113**, 3545–3550. doi:10.1073/pnas.1519994113
- Khan, A., Fornes, O., Stigliani, A., Gheorghe, M., Castro-Mondragon, J. A., van der Lee, R., Bessy, A., Chêneby, J., Kulkarni, S. R., Tan, G. et al. (2018). JASPAR 2018: update of the open-access database of transcription factor binding profiles and its web framework. *Nucleic Acids Res.* **46**, D260–D266. doi:10.1093/nar/gkx1126
- Kim, Y., Kobayashi, A., Sekido, R., Dinapoli, L., Brennan, J., Chaboissier, M.-C., Poulat, F., Behringer, R. R., Lovell-Badge, R. and Capel, B. (2006). Fgf9 and Wnt4 act as antagonistic signals to regulate mammalian sex determination. *PLoS Biol.* **4**, e187. doi:10.1371/journal.pbio.0040187
- Kim, B., Kim, Y., Sakuma, R., Hui, C.-C., Rütther, U. and Jorgensen, J. S. (2011). Primordial germ cell proliferation is impaired in Fused Toes mutant embryos. *Dev. Biol.* **349**, 417–426. doi:10.1016/j.ydbio.2010.10.010
- Kobayashi, D., Kobayashi, M., Matsumoto, K., Ogura, T., Nakafuku, M. and Shimamura, K. (2002). Early subdivisions in the neural plate define distinct competence for inductive signals. *Development* **129**, 83–93.
- Korinek, V., Barker, N., Morin, P. J., VAN Wichen, D., DE Weger, R., Kinzler, K. W., Vogelstein, B. and Clevers, H. (1997). Constitutive transcriptional activation by a beta-catenin-Tcf complex in APC-/- colon carcinoma. *Science* **275**, 1784–1787. doi:10.1126/science.275.5307.1784
- Kumar, M., Camlin, N. J., Holt, J. E., Teixeira, J. M., McLaughlin, E. A. and Tanwar, P. S. (2016). Germ cell specific overactivation of WNT/ $\beta$ -catenin signalling has no effect on folliculogenesis but causes fertility defects due to abnormal foetal development. *Sci. Rep.* **6**, 27273. doi:10.1038/srep27273
- Kuroki, S., Matoba, S., Akiyoshi, M., Matsumura, Y., Miyachi, H., Mise, N., Abe, K., Ogura, A., Wilhelm, D., Koopman, P. et al. (2013). Epigenetic regulation of mouse sex determination by the histone demethylase Jmjd1a. *Science* **341**, 1106–1109. doi:10.1126/science.1239864
- Kuroki, S., Okashita, N., Baba, S., Maeda, R., Miyawaki, S., Yano, M., Yamaguchi, M., Kitano, S., Miyachi, H., Itoh, A. et al. (2017). Rescuing the aberrant sex development of H3K9 demethylase Jmjd1a-deficient mice by modulating H3K9 methylation balance. *PLoS Genet.* **13**, e1007034. doi:10.1371/journal.pgen.1007034
- Lin, R.-S., Jimenez-Movilla, M. and Dean, J. (2014). Figla-Cre transgenic mice expressing myristoylated EGFP in germ cells provide a model for investigating perinatal oocyte dynamics. *PLoS ONE* **9**, e84477. doi:10.1371/journal.pone.0084477
- Liu, C.-F., Bingham, N., Parker, K. and Yao, H. H.-C. (2009). Sex-specific roles of beta-catenin in mouse gonadal development. *Hum. Mol. Genet.* **18**, 405–417. doi:10.1093/hmg/ddn362
- Livak, K. J. and Schmittgen, T. D. (2001). Analysis of relative gene expression data using real-time quantitative PCR and the 2(-Delta Delta C(T)) Method. *Methods* **25**, 402–408. doi:10.1006/meth.2001.1262
- Lovrics, A., Gao, Y., Juhász, B., Bock, I., Byrne, H. M., Dinnyés, A. and Kovács, K. A. (2014). Boolean modelling reveals new regulatory connections between transcription factors orchestrating the development of the ventral spinal cord. *PLoS ONE* **9**, e111430. doi:10.1371/journal.pone.0111430
- Maatouk, D. M., Dinapoli, L., Alvers, A., Parker, K. L., Taketo, M. M. and Capel, B. (2008). Stabilization of  $\beta$ -catenin in XY gonads causes male-to-female sex-reversal. *Hum. Mol. Genet.* **17**, 2949–2955. doi:10.1093/hmg/ddn193
- Maatouk, D. M., Natarajan, A., Shibata, Y., Song, L., Crawford, G. E., Ohler, U. and Capel, B. (2017). Genome-wide identification of regulatory elements in Sertoli cells. *Development* **144**, 720–730. doi:10.1242/dev.142554
- Manuylov, N. L., Smagulova, F. O., Leach, L. and Tevosian, S. G. (2008). Ovarian development in mice requires the GATA4-FOG2 transcription complex. *Development* **135**, 3731–3743. doi:10.1242/dev.024653
- Martineau, J., Nordqvist, K., Tilmann, C., Lovell-Badge, R. and Capel, B. (1997). Male-specific cell migration into the developing gonad. *Curr. Biol.* **7**, 958–968. doi:10.1016/S0960-9822(06)00415-5
- Matsumoto, Y., Buemio, A., Chu, R., Vafaee, M. and Crews, D. (2013). Epigenetic control of gonadal aromatase (cyp19a1) in temperature-dependent sex determination of red-eared slider turtles. *PLoS ONE* **8**, e63599. doi:10.1371/journal.pone.0063599
- McMahon, A. P., Aronow, B. J., Davidson, D. R., Davies, J. A., Gaido, K. W., Grimmond, S., Lessard, J. L., Little, M. H., Potter, S. S., Wilder, E. L. et al. (2008). GUDMAP: the genitourinary developmental molecular anatomy project. *J. Am. Soc. Nephrol.* **19**, 667–671. doi:10.1681/ASN.2007101078
- Morais da Silva, S., Hacker, A., Harley, V., Goodfellow, P., Swain, A. and Lovell-Badge, R. (1996). Sox9 expression during gonadal development implies a conserved role for the gene in testis differentiation in mammals and birds. *Nat. Genet.* **14**, 62–68. doi:10.1038/ng0996-62
- Naillat, F., Prunskaitė-Hyryläinen, R., Pietilä, I., Sormunen, R., Jokela, T., Shan, J. and Vainio, S. J. (2010). Wnt4/5a signalling coordinates cell adhesion and entry into meiosis during presumptive ovarian follicle development. *Hum. Mol. Genet.* **19**, 1539–1550. doi:10.1093/hmg/ddq027
- Naillat, F., Yan, W., Karjalainen, R., Liakhovitskaia, A., Samoylenko, A., Xu, Q., Sun, Z., Shen, B., Medvinsky, A., Quaggin, S. et al. (2015). Identification of the genes regulated by Wnt-4, a critical signal for commitment of the ovary. *Exp. Cell Res.* **332**, 163–178. doi:10.1016/j.yexcr.2015.01.010
- Navarro-Martín, L., Viñas, J., Ribas, L., Díaz, N., Gutiérrez, A., DI Croce, L. and Piferrer, F. (2011). DNA methylation of the gonadal aromatase (cyp19a) promoter is involved in temperature-dependent sex ratio shifts in the European sea bass. *PLoS Genet.* **7**, e1002447. doi:10.1371/journal.pgen.1002447
- Nicol, B. and Yao, H. H.-C. (2014). Building an ovary: insights into establishment of somatic cell lineages in the mouse. *Sex. Dev.* **8**, 243–251. doi:10.1159/000358072
- Parrott, B. B., Kohno, S., Cloy-Mccoy, J. A. and Guille, L. J. (2014). Differential incubation temperatures result in dimorphic DNA methylation patterning of the SOX9 and aromatase promoters in gonads of alligator (*Alligator mississippiensis*) embryos. *Biol. Reprod.* **90**, 2. doi:10.1095/biolreprod.113.111468
- Peters, T., Dildrop, R., Ausmeier, K. and Rütther, U. (2000). Organization of mouse Iroquois homeobox genes in two clusters suggests a conserved regulation and function in vertebrate development. *Genome Res.* **10**, 1453–1462. doi:10.1101/gr.144100
- Piferrer, F. (2013). Epigenetics of sex determination and gonadogenesis. *Dev. Dyn.* **242**, 360–370. doi:10.1002/dvdy.23924

- Sekido, R. and Lovell-Badge, R.** (2008). Sex determination involves synergistic action of SRY and SF1 on a specific Sox9 enhancer. *Nature* **453**, 930-934. doi:10.1038/nature06944
- Sirbu, I. O., Gresh, L., Barra, J. and Duester, G.** (2005). Shifting boundaries of retinoic acid activity control hindbrain segmental gene expression. *Development* **132**, 2611-2622. doi:10.1242/dev.01845
- Svingen, T. and Koopman, P.** (2013). Building the mammalian testis: origins, differentiation, and assembly of the component cell populations. *Genes Dev.* **27**, 2409-2426. doi:10.1101/gad.228080.113
- Tomizuka, K., Horikoshi, K., Kitada, R., Sugawara, Y., Iba, Y., Kojima, A., Yoshitome, A., Yamawaki, K., Amagai, M., Inoue, A. et al.** (2008). R-spondin1 plays an essential role in ovarian development through positively regulating Wnt-4 signaling. *Hum. Mol. Genet.* **17**, 1278-1291. doi:10.1093/hmg/ddn036
- Uhlenhaut, N. H., Jakob, S., Anlag, K., Eisenberger, T., Sekido, R., Kress, J., Treier, A.-C., Klugmann, C., Klasen, C., Holter, N. I. et al.** (2009). Somatic sex reprogramming of adult ovaries to testes by FOXL2 ablation. *Cell* **139**, 1130-1142. doi:10.1016/j.cell.2009.11.021
- Usongo, M., Rizk, A. and Farookhi, R.** (2012).  $\beta$ -Catenin/Tcf signaling in murine oocytes identifies nonovulatory follicles. *Reproduction* **144**, 669-676. doi:10.1530/REP-12-0291
- Vainio, S., Heikkilä, M., Kispert, A., Chin, N. and McMahon, A. P.** (1999). Female development in mammals is regulated by Wnt-4 signalling. *Nature* **397**, 405-409. doi:10.1038/17068
- van de Wetering, M., Cavallo, R., Dooijes, D., VAN Beest, M., VAN Es, J., Loureiro, J., Ypma, A., Hursh, D., Jones, T., Bejsovec, A. et al.** (1997). Armadillo coactivates transcription driven by the product of the *Drosophila* segment polarity gene dTCF. *Cell* **88**, 789-799. doi:10.1016/S0092-8674(00)81925-X
- van Galen, P., Viny, A. D., Ram, O., Ryan, R. J. H., Cotton, M. J., Donohue, L., Sievers, C., Drier, Y., Liao, B. B., Gillespie, S. M. et al.** (2016). A multiplexed system for quantitative comparisons of chromatin landscapes. *Mol. Cell* **61**, 170-180. doi:10.1016/j.molcel.2015.11.003
- Yan, M., Li, G. and An, J.** (2017). Discovery of small molecule inhibitors of the Wnt/ $\beta$ -catenin signaling pathway by targeting  $\beta$ -catenin/Tcf4 interactions. *Exp. Biol. Med. (Maywood)* **242**, 1185-1197. doi:10.1177/1535370217708198
- Yan, H., Wen, J., Zhang, T., Zheng, W., He, M., Huang, K., Guo, Q., Chen, Q., Yang, Y., Deng, G. et al.** (2019). Oocyte-derived E-cadherin acts as a multiple functional factor maintaining the primordial follicle pool in mice. *Cell Death Dis.* **10**, 160. doi:10.1038/s41419-018-1208-3

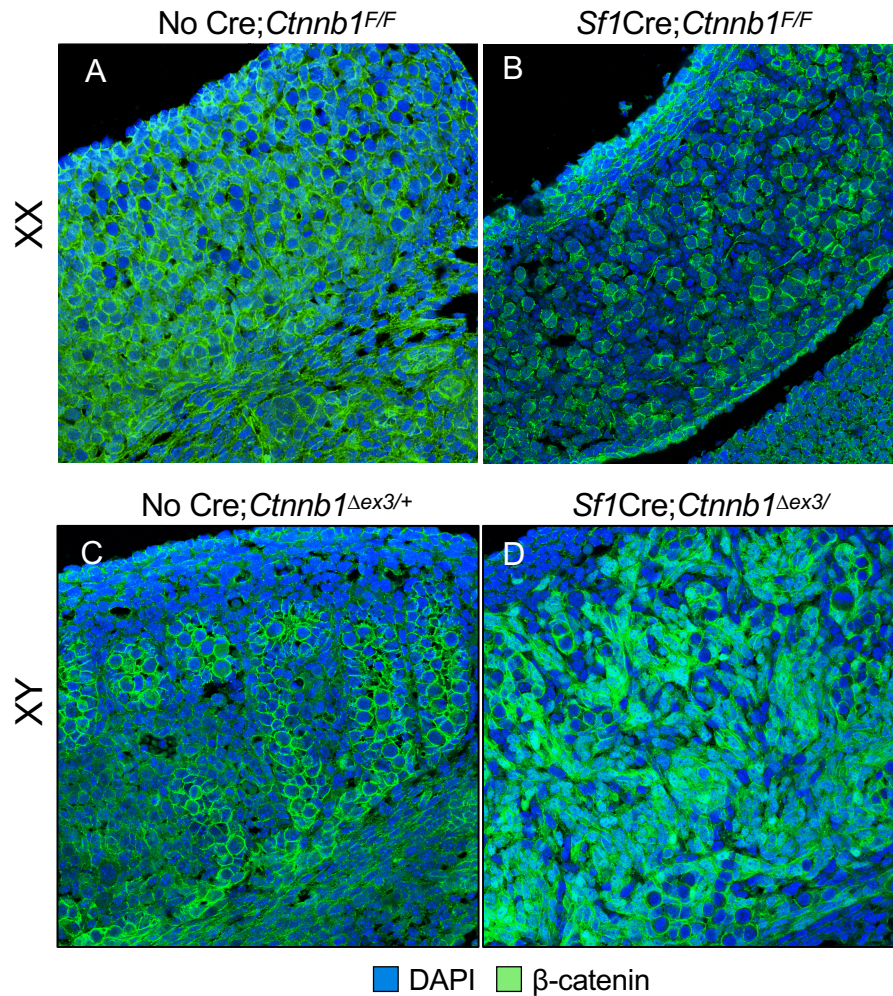


**Figure S1:** Somatic cell manipulation of  $\beta$ -catenin in the developing gonad E14.5 (A) Control ovary (No Cre;*Ctnnb1*<sup>F/F</sup>) and (B) mutant ovary (Sf1Cre;*Ctnnb1*<sup>F/F</sup>)  $\beta$ -catenin green, DAPI blue. The remaining  $\beta$ -catenin in the mutant ovary resides in the germ cell membrane. E14.5 (C) Control testis (No Cre;*Ctnnb1*<sup>Δex3/+</sup>) and (D) mutant testis (Sf1Cre;*Ctnnb1*<sup>Δex3/+</sup>)  $\beta$ -catenin green, DAPI blue.  $\beta$ -catenin is highly stabilized in the mutant testis.



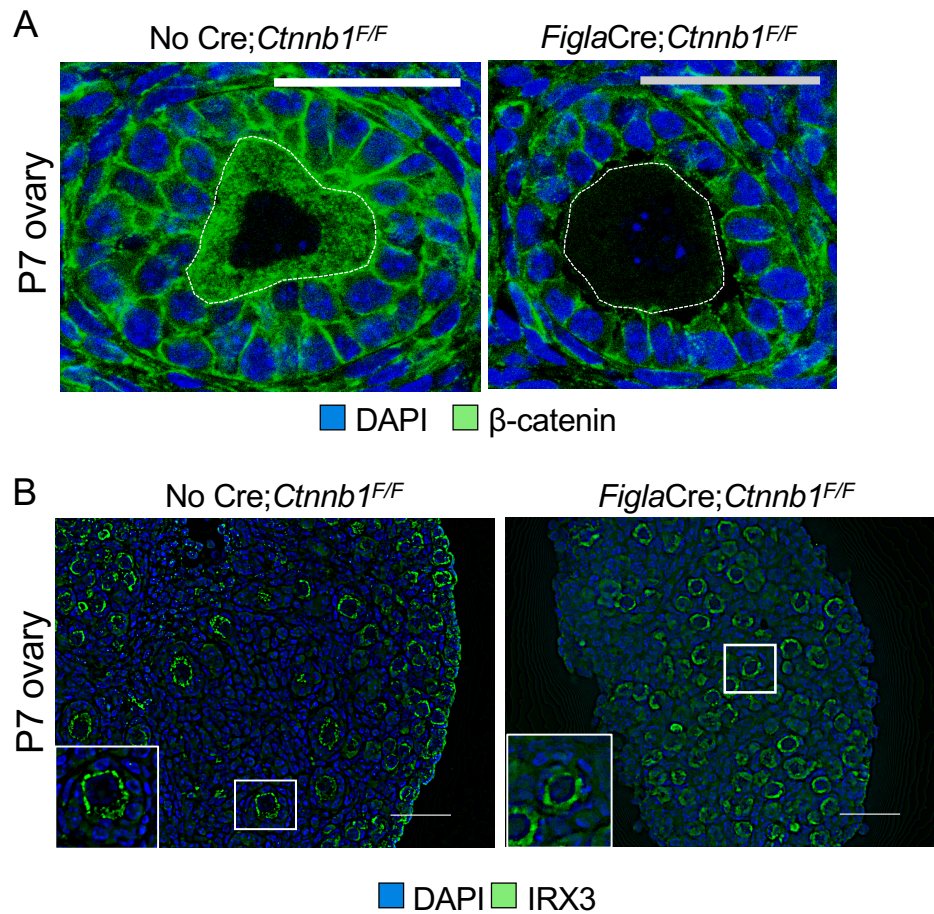


**Figure S2:** *FiglaCre* targeted loss of  $\beta$ -catenin does not affect *IRX3* expression in oocytes

(**A**) Immunofluorescence image of a primary/transitioning follicle in a P7 ovary showing that  $\beta$ -catenin is knocked out specifically in the oocyte. No Cre; *Ctnnb1*<sup>F/F</sup> (control, left panel). *FiglaCre*; *Ctnnb1*<sup>F/F</sup> (mutant, right panel). DAPI (blue) and  $\beta$ -catenin (green), White dotted lines outline the membrane of the germ cell. (**B**) IHC images of P7 ovaries for DAPI (blue) and *IRX3* (green). No difference was observed in *IRX3* staining between the oocytes of the control and mutant ovaries, including growing follicles (inset). Timing starting at secondary follicles is consistent with the onset of transcriptional activity of  $\beta$ -catenin in postnatal ovaries as reported by Usongo *et al.* 2012. Scale bars set to 50  $\mu$ m.



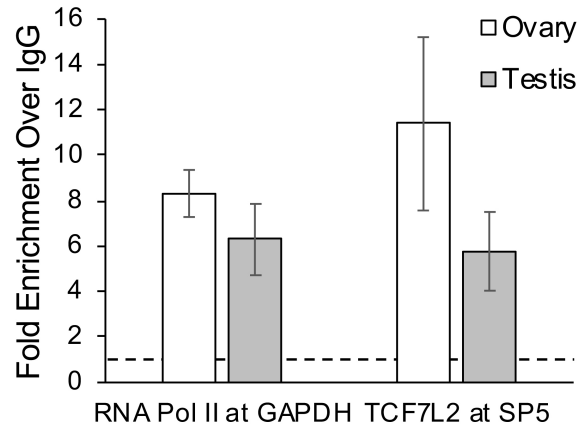


**Figure S3: Chromatin Immunoprecipitation controls**  
 RNA Pol II is enriched at the GAPDH promoter and  
 TCF7L2 is enriched at the SP5 promoter in both  
 ovaries and testes

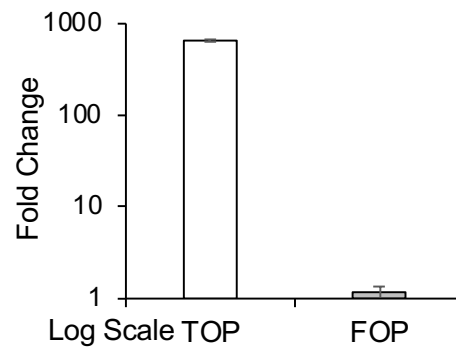


**Figure S4:** Validation of  $\beta$ -catenin specific responsiveness for CMV-S37A expression vector. TOPflash and FOPflash constructs were co-transfected with 50ng/well CMV-EGFP or CMV-S37A and normalized to pGL3Basic. Only TOPflash co-transfected with CMV-S37A showed a specific and robust increase in luciferase expression.

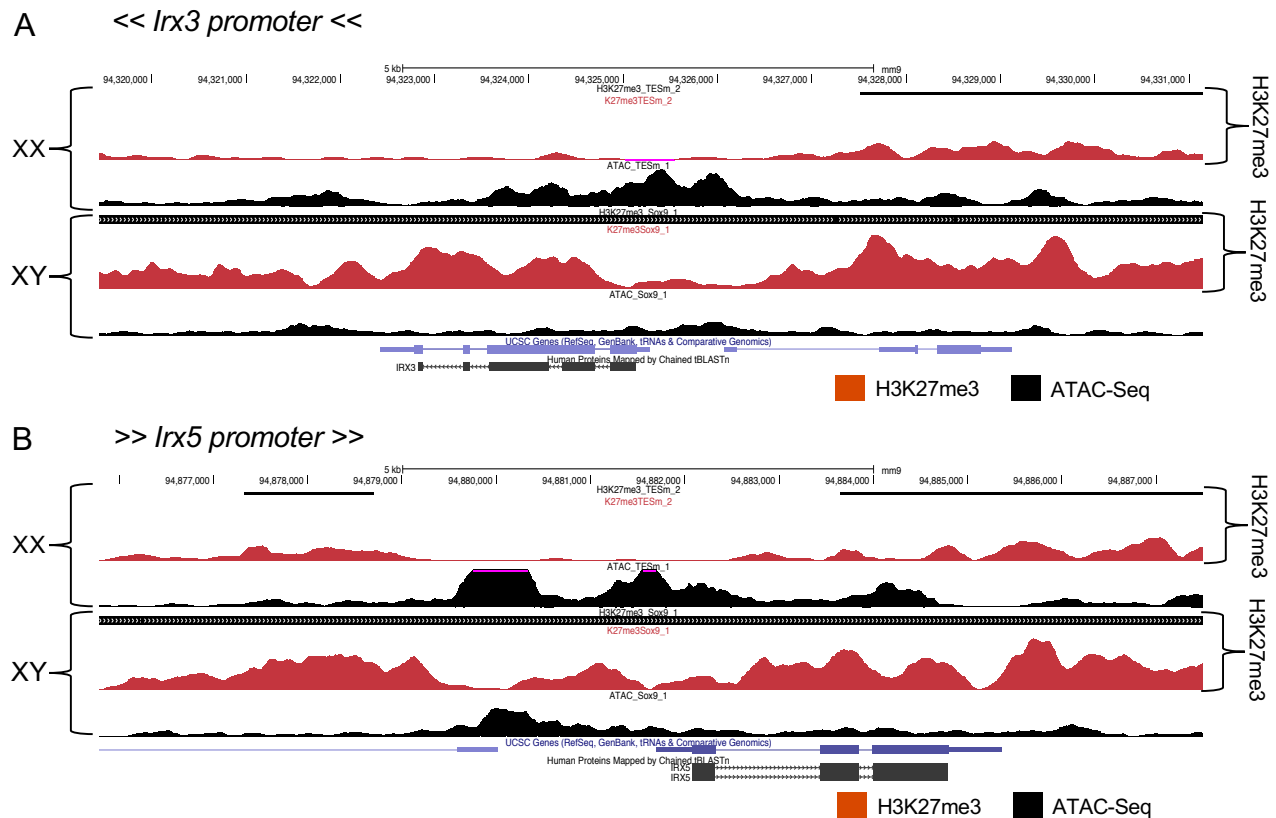


**Figure S5: Epigenetic marks on *Irx3* and *Irx5* promoters**

H3K27me3 (red peaks and back solid lines) and open chromatin sites (ATAC-Seq, black peaks) are shown for *Irx3* (C) and *Irx5* (D) promoters in male and female somatic cell populations. Arrows in label match the direction for coding sequences of each gene. ATAC-Seq peaks are enriched while there is a paucity of H3K27me3 peaks in XX samples. Black bars represent regions of significant enrichment when compared to flanking regions as determined by HOMER, thicker lines represent increased enrichment. Black bars are absent in both proximal promoter regions in XX samples.

Site Label	Forward Primer		Reverse Primer	Total insert length
+205kb	5'- GCGCGGTACCTCACCTGGTAACTTTGT GCTGT-3'		5'- GCGCCTCGAGCCAAGGCTTCCGGT ATCAGC-3'	108bp
+86kb	5'- GCGCGGTACCTTCCCTTTCTATTTGTT CAGAAG-3'		5'- GCGCCTCGAGTTCCTCGGCTGAC AGAG-3'	59bp
-305AB kb	5'- GCGCGGTACCGGTTTCAAAAAGCCCAA GTG-3'		5'- GCGCCTCGAGTTATTTCTCTCTTTC TCTCTCTCCA-3'	250bp
-580kb	5'- GCGCGGTACCCCGCCATGATAGGAGT CAAC-3'		5'- GCGCCTCGAGGGCAGCCCTTTGTA AATGTT-3'	89bp
Mutation Site	+205kb	+86kb	-305kb (AB)	-580kb
Wild Type Sequence	GTTCAAAGGC	GTTCAAAGCG	(A) GTTCAAAGTC (B) TTTCAAAGGG	CATCAAAGAC
Mutated Sequence	GT <b>C</b> CAAAGGC	GT <b>C</b> CAAAGCG	(A) GT <b>C</b> CAAAGTC (B) TT <b>C</b> CAAAGGG	CA <b>C</b> CAAAGAC

**Table S1:** Individual potential enhancer sites containing TCF/LEF motif were cloned into the pGL3 Basic backbone using KpnI and XhoI. Primer sequences listed above and the insert size. DNA was generated by PCR with mouse genomic DNA. Wild type and mutated TCF/LEF binding motif for each enhancer site. The mutated base pair is in bold.



**Supplementary Table S2:** Real-time qPCR primer sequences

Gene	Forward Primer	Reverse Primer
<i>36B4</i>	5' – CGACCTGGAAGTCCAACTAC – 3'	5' – ATCTGCTGCATCTGCTTG – 3'
<i>Gapdh</i>	5' – TTCACCACCATGGAGAAGGC – 3'	5' – GGCATGGACTGTGGTCATGA – 3'
<i>Rps29</i>	5' - TGAAGGCAAGATGGGTCAC - 3'	3' - GCACATGTTGAGCCCGTATT - 5'
<i>Axin2</i>	5' – CCAGGCTGGAGAACTGAACT - 3'	5' – CCTGCTCAGACCCCTCCTTT - 3'
<i>Fst</i>	5' - AAAACCTACCGCAACGAATG - 3'	5' - TTCAGAAGAGGAGGGCTCTG - 3'
<i>Bmp2</i>	5' – CGGACTGCGGTCTCCTAA – 3'	5' – GGGGAAGCAGCAACACTAGA – 3'
<i>Irx3</i>	5' - CGCCTCAAGAAGGAGACAAGA - 3'	5' - CGCTCGCTCCCATAAGCAT - 3'
<i>Irx5</i>	5' - GGCTACAACCTCGCACCTCCA - 3'	5' - CCAAGGAACCTGCCATACCG - 3'